



Published in final edited form as:

*Nat Biomed Eng.* 2017 ; 1: . doi:10.1038/s41551-016-0008.

## Light in diagnosis, therapy and surgery

Seok Hyun Yun<sup>1,2,3,\*</sup> and Sheldon J. J. Kwok<sup>1,3</sup>

<sup>1</sup>Wellman Center for Photomedicine, Massachusetts General Hospital, 65 Landsdowne Street, Cambridge, MA 02139, USA

<sup>2</sup>Department of Dermatology, Harvard Medical School, 25 Shattuck Street, Boston, MA 02115

<sup>3</sup>Harvard–MIT Health Sciences and Technology, 77 Massachusetts Avenue, Cambridge, MA 02139, USA

### Abstract

Light and optical techniques have made profound impacts on modern medicine, with numerous lasers and optical devices being currently used in clinical practice to assess health and treat disease. Recent advances in biomedical optics have enabled increasingly sophisticated technologies — in particular those that integrate photonics with nanotechnology, biomaterials and genetic engineering. In this Review, we revisit the fundamentals of light–matter interactions, describe the applications of light in imaging, diagnosis, therapy and surgery, overview their clinical use, and discuss the promise of emerging light-based technologies.

---

The modern use of light in medicine began in the 19<sup>th</sup> century, with rapid improvements in the understanding of both the physical nature of light and fundamental light–matter interactions. A notable example of an early triumph in phototherapy is the ultraviolet (UV) induced treatment of *lupus vulgaris* invented by physician Niels Finsen, who in 1903 was awarded the Nobel Prize in Physiology and Medicine for this application. Since 1960, the development of lasers has opened new medical avenues. Today, numerous laser-based therapeutic and diagnostic devices are routinely used in the clinic.

Within tissue, photons interact with biological matter via various processes, which can be broadly categorized into scattering and absorption (Fig. 1a and Box 1). Scattering can alter the propagation path, polarization and spectrum of scattered light. The states of the scattered light can be analysed and mapped for diagnosis and imaging. In light absorption, the energy of photons is converted to electronic or vibrational energy in the absorbing molecule. Some of that energy can be re-emitted through luminescence (for example, fluorescence), inelastic scattering, or acoustomechanical waves. Such emission from the tissue carries the information about its microstructure and molecular contents, and serves as the basis for

---

Users may view, print, copy, and download text and data-mine the content in such documents, for the purposes of academic research, subject always to the full Conditions of use: [http://www.nature.com/authors/editorial\\_policies/license.html#terms](http://www.nature.com/authors/editorial_policies/license.html#terms)

\* syun@hms.harvard.edu.

S.H.Y. and S.J.J.K. designed and wrote the manuscript.

#### Competing financial interests

The author declares no competing financial interests

optical diagnostics and imaging. On the other hand, the photoexcitation of intrinsic molecules or exogenous light-sensitive agents introduced in the body can give rise to various effects to the tissue and cells within it, via the generation of heat (photothermal), chemical reactions (photochemical), and biological processes (photo-biological or optogenetic). Optical therapy and laser surgery use these effects in a controlled manner.

## BOX 1

### Light–tissue interactions

Different diagnostic and therapeutic applications of light require a specific optimal choice of optical parameters, including wavelength  $\lambda$ , exposure time  $\tau$ , beam area  $A$ , energy  $E$ , power  $P = E/\tau$ , intensity  $P/A$  and fluence  $E/A$  (Fig. 1b).

#### Light scattering

Elastic light scattering occurs due to inhomogeneous electric polarization density in tissues. The magnitude of Rayleigh scattering from atoms and molecules is proportional to  $1/\lambda^4$ , and Mie-type scattering due to microscopic index variations is nearly independent of  $\lambda$ . The experimentally measured ‘reduced’ scattering coefficients fit well with  $a*\lambda^{-b}$ , where  $b$  ranges from 0.7 to 1.6 and  $a$  varies from 19 to 79  $\text{cm}^{-1}$ , depending on tissue type<sup>235</sup>. Inelastic light scattering arises from time-varying scatters (dynamic light scattering), thermodynamically produced hypersonic waves (Brillouin scattering) and molecular vibrations (Raman scattering). The scattering coefficients for spontaneous inelastic scattering are several orders of magnitude lower than those for elastic scattering.

#### Penetration depths

Scattering and absorption limit how far light can diffuse into tissue. In skin tissues, the effective penetration depth at which the incident optical energy drops to  $1/e$  (~37%) is typically 50–100  $\mu\text{m}$  for UV and blue light ( $\lambda=400\text{--}450\text{ nm}$ ) and also for infrared light above 2000 nm because of high light absorption by water. The penetration depth of green light (500–550 nm) is a few hundreds of micrometres, limited by light absorption by melanin and haemoglobin. The penetration is the largest, typically 1–3 mm, for red and NIR light (600–1350 nm).

#### Photothermal effects

Laser absorption by tissue increases its local temperature. Hyperthermia arises at 42.5–43.0 °C, tissue coagulation and welding occurs typically at 60–70 °C, and higher temperatures lead to tissue ablation via vaporization (100 °C) and carbonization (300–450 °C). The required energy depends on the desired temperature, light penetration, and target tissue volume. Without heat dissipation, it takes approximately 4 J (heat capacity) to increase the temperature of 1  $\text{cm}^3$  of tissue by 1 °C, and ~2.7 kJ (latent heat of water) to vaporize the water in the tissue. For example, when a laser beam with a short penetration depth of 100  $\mu\text{m}$  is illuminated over an area of 1  $\text{cm}^2$ , a fluence of 1  $\text{J}/\text{cm}^2$  will raise the temperature of the tissue surface by 25 °C above body temperature (62 °C), at which protein denaturation occurs. A fluence of 25  $\text{J}/\text{cm}^2$  would heat and vaporize the 100- $\mu\text{m}$ -thick layer of tissue to 100 °C and thereby ablate it.

Pulsed irradiation is commonly used to avoid heat diffusion during irradiation and to minimize collateral tissue damage. For ablation of large tissue volumes, pulse widths of 1–100 ms are adequate; for high-precision ablation, micro- and nanosecond pulses are needed. The thermal diffusion length,  $(4\alpha\tau)^{1/2}$ , where  $\alpha \approx 1.4 \times 10^{-7} \text{ cm}^2 \text{ s}^{-1}$  is the heat diffusivity in tissue, is 1.2 mm for continuous-wave (cw) illumination for  $\tau = 10 \text{ s}$ , yet only 37 nm for short pulses with  $\tau = 10 \text{ ns}$ . The peak temperature at which irreversible tissue damage occurs depends on exposure time: according to the Arrhenius model<sup>236</sup>, protein denaturation is induced at 60 °C for  $\tau = 1 \text{ s}$  but requires 90 °C for  $\tau = 10 \text{ ns}$ .

#### Photomechanical effects

In tissue, localized absorption of short laser pulses ( $< 1 \mu\text{s}$ ) gives rise to a local rise in pressure ( $\sim 800 \text{ kPa per } ^\circ\text{C}$ ), which generates propagating stress waves with acoustic energy increasing with the square of optical pulse energy. For diagnosis, low optical intensity is used, which limits the temperature rise to less than 1 °C, and generated ultrasound waves are detected for mapping the concentration of light-absorbing molecules. At high optical intensity, shock waves can cause mechanical disruption, often of enough intensity to fragment kidney stones. Photoablation by pulsed excimer (or exciplex) laser involves molecular bond breakage by intense UV light, followed by mechanical ejection of the tissue<sup>237</sup>. And femtosecond mode-locked laser pulses ( $\sim 100 \text{ fs}$ ) focused to a small spot size at high intensity can generate plasma (that is, ionized gas) at extremely high temperature — a process known as optical breakdown — that can ablate tissue and make a clean cut with negligible collateral thermal damage through complex processes that involve mechanical ejection of tissue.

#### Photochemical/photobiological effects

Upon absorbing a photon, an excited molecule can interact with a neighbouring molecule to cause photochemical effects, such as the generation of reactive radicals (ROS) and singlet oxygen, as well as photobiological effects, such as the destruction of enzymes in cellular signalling pathways, the opening of ion channels, and the promotion of specific gene expression. Although this process involves one photon per molecule, a large number of photons are needed: the number is approximately equal to  $A/\sigma_a$ , where  $\sigma_a$  is the molecule's absorption cross-section (which is easily determined from a molar extinction measurement). Most light-absorbing organic molecules have peak extinction coefficients of  $10^4\text{--}10^5 \text{ M}^{-1}\text{cm}^{-1}$ . For example, the peak extinction coefficient for human rhodopsin is  $40,000 \text{ M}^{-1}\text{cm}^{-1}$  at 493 nm, and therefore  $\sigma_a = 2 \times 10^{-16} \text{ cm}^2$ . The average optical fluence required to excite one rhodopsin molecule (at 63% probability) is  $E_p/\sigma_a = 2 \text{ mJ/cm}^2$ , where  $E_p$  is the photon energy. Although optical fluence in the order of 1–10  $\text{mJ/cm}^2$  is sufficient for photoexcitation *in vitro*, in tissue a higher optical energy is necessary to compensate for optical loss. Furthermore, the typical efficiency (quantum yield) of a photochemical reaction ranges from 10% to 80%, and a molecule may be excited multiple times to enhance the photochemical effect. For this reason, the optimal dose required in medical applications often exceeds  $1 \text{ J/cm}^2$ . At this level, photothermal tissue damage is minimal ( $< 2.5 \text{ }^\circ\text{C}$ ) when visible or NIR light with a penetration depth longer than 1 mm is used.

#### Safety limits for diagnosis and imaging

Diagnostic applications demand low optical powers for safety. For optical radiation, the requirement is quantified in terms of the maximum permissible exposure (MPE), which is defined as one tenth of the damage threshold resulting from photothermal and photochemical effects. According to the standard guideline<sup>238</sup>, laser-exposure limits for the skin are given as  $0.02C_A \text{ J/cm}^2$  for  $\tau=1-100 \text{ ns}$ , and  $1.1 C_A \tau^{0.25} \text{ J/cm}^2$  for  $\tau=100 \text{ ns}$  to  $\tau=10 \text{ s}$  (where the empirical coefficient  $C_A$  is 1 for  $\lambda=400-700 \text{ nm}$  and increases to 5 for  $\lambda=1050-1400 \text{ nm}$ ). For exposures of  $\tau>10 \text{ s}$ , MPE is  $2C_A \text{ W/cm}^2$  (in this case MPE is given in intensity units because thermal equilibrium is reached between laser-induced heating and conductive cooling).

X-rays and gamma rays have transformed modern medicine by enabling computed tomography (CT) and positron emission tomography (PET), as well as radiation therapy. Radio waves and magnetic fields have made magnetic resonance imaging (MRI) possible. Among the wide spectrum of electromagnetic waves, light comprises a region from the deep blue to the near infrared (NIR) and provides a distinct advantage due to its unique photon energy range of 0.5–3 eV. These energies fall into a window that permits rich yet safe interactions with organic molecules. At higher energies, bond dissociation (>3.6 eV for C–C and C–H bonds) and ionization (>7 eV) can occur, and at lower energies, water absorption dominates, preventing any specific targeting of molecules. Light-based technologies in medicine take advantage of the variety of light–molecule interactions in this optical window (Box 2).

## BOX 2

### Why light for medicine?

Plants have sophisticated energy-harvesting machinery to convert solar energy, highest in the 400–700 nm spectral range<sup>239</sup>, into chemical energy. Microorganisms, such as green algae, have light-gated ion channels that enable phototaxis and thus enhanced energy harvest. The vision system of higher organisms is based on phototransduction proteins, which help the organisms search for food and keep away from danger. Fruit flies and jellyfish generate bioluminescence, and insects and birds reflect colorful irradiance with photonic crystal structures for improved survival and reproduction. These examples illustrate not only the extraordinary connection between light and biology, but also the role of light as an important determinant and driving force of natural evolution.

The use of light in medicine is an extension of light's evolutionary role in biology. Color perception is mediated by the absorption of light by three types of cones (blue, green and red, with respective wavelengths of 400–450 nm, 500–570 nm and 610–750 nm). Yet various types of light–tissue interactions generate contrast beyond what can be perceived by the naked eye, enabling molecular imaging of cells and tissues at high resolutions. The therapeutic effects of light on tissues can be traced to the absorption of specific wavelengths by a variety of light-sensitive molecules that are endogenously present in the human body or may be inserted via gene-editing technologies. Most likely, medicine will benefit from increasingly sophisticated light-based technologies that use materials and machineries resulting from billions of years of evolution.

In what follows, we overview the major applications of light in three categories: optical diagnosis, laser surgery and light-activated therapy (Fig. 2a). We also discuss optical imaging, which plays important roles in diagnosis, surgery guidance and therapy monitoring. For each technology, we briefly highlight its principle of operation, advantages and limitations, and current clinical utilities. We then describe emerging light-based technologies, with particular emphasis on opportunities in nanomedicine, optogenetics and implantable devices.

## Laser surgery

The development of lasers expanded the therapeutic applications of light well beyond the long-known effects of sunlight and focused lamps. With lasers, emission intensities can be several orders of magnitude higher than that of sunlight, short pulses are readily generated, and wavelengths can be precisely selected. Physicians started exploring the medical applications of lasers after the first demonstration of the ruby laser by Maiman in 1960, when biohazards of high-intensity laser pulses to the eye and skin became appreciated. Photocoagulation in the retina<sup>1</sup>, destruction of skin lesions<sup>2</sup> and removal of dental caries and cardiovascular plaques are examples of early pioneering works. Today, medical lasers are routinely used in many applications, including surgeries in ophthalmology, the treatment of cutaneous disorders, and tissue ablation in internal organs through fibre-optic delivery. This has led to a global market for therapeutic lasers estimated to be over \$3 billion (Figs. 2b and 2c).

### Laser surgery in ophthalmology

The ablative ability of UV photons from an ArF excimer laser (193 nm) to reshape the cornea is widely used for refractive error correction<sup>3</sup>. UV radiation breaks the peptide bonds of collagen fibres within the cornea, expelling a discrete volume of corneal tissue from the surface<sup>4</sup> (Fig. 3a). For example, a single excimer pulse (0.25 J/cm<sup>2</sup>) with a spot size of 1 mm removes about 0.25  $\mu\text{m}$  of tissue. A customized scanning pattern generated by optical wavefront analysis of the patient is used to precisely reshape the patient's cornea. Unlike photorefractive keratectomy (PRK), where the corneal epithelium is irradiated, laser-assisted *in-situ* keratomileusis (LASIK) ablates corneal stroma through a ~160- $\mu\text{m}$ -thick corneal flap that is prepared by using femtosecond Nd:glass laser pulses (600 fs; 1053 nm) focused to a spot size of 2–3  $\mu\text{m}$ . Millions of LASIK procedures have been performed in the past two decades, with a 95.4% overall patient satisfaction in a recent metaanalysis<sup>5</sup>. Laser thermal keratoplasty uses holmium:YAG (2100 nm) laser energy to reshape the cornea but is less used due to plastic regression after treatment.

A cataract in the lens is the leading cause of preventable blindness worldwide; in fact, over 20 million cataract surgeries are performed annually. In these, a laser is used to create an incision on the lens capsule and gain access to the cataract. Nd:YAG laser capsulotomy is used to treat posterior capsule opacification, which occurs in about 20% of patients following cataract surgery. Although the disruption of the crystalline lens is done by ultrasound, femtosecond laser technology for cataract surgery may offer a more reliable and improved safety profile<sup>6</sup>.

Laser coagulation therapy is a common procedure to seal a retinal tear or small retinal detachment<sup>7</sup> (Fig. 3b), shrink abnormal blood vessels in proliferative diabetic retinopathy, and seal blood vessels in retinal edema<sup>8</sup>. Green and yellow wavelengths, well absorbed by oxyhemoglobin and melanin, are suitable for photocoagulation. Typically, this procedure uses a potassium titanyl phosphate (KTP)-based frequency-doubled Nd:YAG (532 nm), Krypton ion laser (531 or 568 nm), or a diode-pumped dye laser (577 nm) at a typical fluence of 100 J/cm<sup>2</sup> and duration of 10–100 ms per pulse.

### Dermatological and aesthetic treatments

Since the laser was invented, efforts have been made to develop more effective lasers for the removal of unwanted skin markings, including tattoos, birth marks, stretch marks, port-wine stains, acne scars and leg veins<sup>9</sup>. Cutaneous laser surgery was revolutionized by the concept of selective photothermolysis<sup>10</sup>, which states that optical pulses with optimal parameters — wavelength, duration, beam size and energy — can selectively destruct a target within the skin, minimizing the risk of scarring and damage to normal tissue. Pulsed dye laser (PDL) tuned at 585 nm (0.4–2 ms; 5–10 J/cm<sup>2</sup>) removes skin markings by selectively targeting haemoglobin within red blood cells, with minimal thermal damage to other structures<sup>11</sup>. Spot sizes of 2–10 mm are used to permit deeper dermal penetration and the destruction of larger blood vessels. PDL is useful in the treatment of port-wine stains, superficial haemangiomas and other vascular lesions. A cryogen-cooling device is used to limit the temperature rise at the surface of the skin while allowing heat accumulation at the target region underneath<sup>12</sup>. PDL is also used to treat non-vascular lesions such as hypertrophic scars, keloids and striae.

Laser skin resurfacing can reduce facial wrinkles, scars and pimples. Indeed, ablative therapy using CO<sub>2</sub> lasers (10.6 μm; 1–10 ns; 5 J/cm<sup>2</sup>) is the current gold standard<sup>13</sup>. Yet the Er:YAG laser (2940 nm) has a higher water absorption (12,800 cm<sup>-1</sup>) than the CO<sub>2</sub> laser (800 cm<sup>-1</sup>), ablating 5–20 μm of tissue at 5 J/cm<sup>2</sup>. Alternatively, non-ablative resurfacing can minimize risk and shorten recovery times by producing dermal thermal injury to reduce rhytides (skin wrinkles) and photodamage while preserving the epidermis. Moreover, fractional resurfacing thermally coagulates or ablates microscopic columns of epidermal and dermal tissue in a regularly spaced array that is followed by rapid re-epithelization and dermal remodelling, which reduces the risk of scarring, improves treatment efficacy and shortens recovery time<sup>14</sup>. Fractionated lasers are divided into non-ablative NIR lasers (typically, 1550 nm)<sup>15</sup> and ablative infrared lasers (typically, 10.6 μm)<sup>16</sup> (Fig. 3c).

When targeting melanin, laser treatment can lighten or remove benign epidermal and dermal pigmented lesions as well as tattoos. To induce rapid ablative heating, nanosecond Q-switched pulses (10–100 ns; 3–7 J/cm<sup>2</sup>; 1–10 Hz) are the usual choice. The optimal laser wavelength depends on specific skin types, target depth and pigment absorption. Q-switched Ruby (694 nm), Alexandrite (755 nm), and Nd:YAG (1064 nm) lasers are typically used<sup>17</sup>. Superficial lesions are treated with shorter wavelengths (510 nm for PDL; 532 nm for KTP). Also, a picosecond Alexandrite laser has been developed for targeting smaller pigments<sup>18</sup>.

Laser hair removal uses pulses targeting melanin in the hair shaft and hair follicle to achieve long-lasting removal of excessive hairs in cosmetically undesirable locations<sup>19</sup>. Because of



the presence of melanin in the epidermis, active cooling of the skin by spray or contact cooling is critical to minimize unwanted thermal injury of the tissue. A variety of lasers emitting long pulses (1–600 ms; 10–50 J/cm<sup>2</sup>), such as the Ruby laser, the Alexandrite laser, semiconductor diode lasers (800–810 nm), and flash lamp-based intense pulsed light (IPL) sources (550–1200 nm) are suited for photoepilation.

Recently, a number of hand-held light sources have become available as consumer cosmetic products for home use in applications including photorejuvenation, hair growth, hair removal, and acne treatment<sup>20</sup>. Advances in compact fibre lasers in the NIR range may also replace some of the existing solid-state Nd:YAG and holmium:YAG lasers used in the clinic<sup>21</sup>.

### **Laser surgery in urology and gastroenterology**

Benign prostate hyperplasia (BPH) is a non-cancerous condition, affecting about 50% of men by the age of 50 and up to 90% older than 80, in which an enlarged prostate squeezes or partially blocks the surrounding urethra. High-power laser (80–180 W; 20 ms; 400 J/cm<sup>2</sup>) is used to remove the excess tissue. Holmium-laser enucleation or ablation of the prostate<sup>22</sup>, developed in the 1990s, is less popular compared to transurethral resection using electrical loops. A rapidly growing laser-surgery technique for the prostate is photoselective vaporization using a frequency-doubled Nd:YAG laser (532 nm) delivered fibre-optically through a cystoscope<sup>23</sup> (Fig. 3d). Medicare estimated that ~72,000 photoselective vaporization procedures were performed in the United States in 2008, accounting for 27% of all benign prostate-hyperplasia surgeries, while transurethral resection amounted to 64% of them.

Lithotripsy is a surgical procedure to remove stones from the urinary tract (kidney, ureter, bladder or urethra) in patients with urinary calculi (stones). When ultrasound-based shock-wave lithotripsy cannot be used, lithotripsy is performed using a holmium:YAG laser through a flexible ureteroscope<sup>24</sup>. Laser lithotripsy is also used for the fragmentation of intraductal gallstones, particularly stones that cannot be targeted by conventional mechanical lithotripsy<sup>25</sup>.

### **Lasers in cardiology and vascular surgery**

Laser-assisted lead extraction is a highly effective procedure for the extraction of lead wires of cardiac pacemakers and defibrillators from coronary blood vessels<sup>26</sup>. This method uses a special sheath that conducts laser pulses to the distal tip as a ring of light to break up scar tissue around the lead, facilitating removal. Typically, XeCl laser pulses (100–200 ns; 3–6 J/cm<sup>2</sup>) are used, causing localized ablation of the ~100 µm of tissue in front of the tip<sup>27</sup>.

An early approach for angioplasty in the treatment of coronary artery disease was excimer laser ablation of plaques through a fibre-optic catheter<sup>28</sup>. However, its use has declined in recent years. Endovenous laser treatment is effective for treating lower-extremity venous insufficiency such as great saphenous vein reflux<sup>29</sup>. High-power laser light, typically from cw NIR diode lasers (810, 940, or 1470 nm; 10–30 W), is intravenously delivered through a fibre-optic to ablate the varicose veins<sup>30</sup>. For asymptomatic lower-extremity telangiectasias,

lasers (Nd:YAG, diode, KTP) are applied externally, particularly when sclerotherapy is not feasible<sup>31</sup>.

### Other applications

Various dental lasers have been used to remove and modify soft and hard tissues in the oral cavity. For instance, CO<sub>2</sub>, Nd:YAG and diode lasers are used for soft-tissue removal such as gingivectomy, for killing bacteria, and for promoting the regrowth of tissues. Applications to hard tissue (enamel and dentin), such as dental drilling using highly ablative Er:YAG lasers<sup>32</sup>, are also growing<sup>33</sup>.

In otolaryngology, the CO<sub>2</sub> laser is routinely used because of its minimal lateral tissue damage particularly in larynx surgery<sup>34</sup>. Interstitial laser coagulation has shown potential for causing necrosis of small tumour metastases<sup>35</sup>. Endoscopic laser therapy can be used for the palliation of advanced esophageal cancers<sup>36</sup>. And Nd:YAG lasers are used in bronchoscopic laser resection to relieve intraluminal airway obstruction caused by bronchogenic carcinoma or foreign bodies<sup>37</sup>.

### Light-activated therapies

Light-activated therapeutic applications harness the versatility of light in manipulating photoactive molecules, proteins and cells. Phototherapies, which require only an appropriately selected light source, are commonplace in the clinic and are first-line treatments for some conditions. For instance, since the 1960s blue-light phototherapy has been used to treat severe hyperbilirubinemia in millions of infants<sup>38</sup>. More broadly, the use of exogenous photosensitizers offers capabilities beyond intrinsic light-induced signalling, such as oxidative killing of unwanted cells in photodynamic therapy (PDT). Today, PDT is an established modality used in oncology, dermatology, ophthalmology, dentistry, cosmetics and other fields. The combined global markets for drugs and devices used in phototherapy and photodynamic therapy are estimated to be \$630 million in 2014 (Fig. 2b). Recent innovations in nanomedicine have enabled the development of multimodal nanocarriers with numerous light-activated functions, including conversion of NIR to visible light, photodynamic and photothermal therapies, drug delivery and imaging. Optogenetics represents a new frontier in light-activated therapies, enabling unprecedented control over neural activity and cellular signalling.

### Ultraviolet light (100–400 nm)

Exposure to the sun's UV radiation, consisting of 95% UVA (320–400 nm) and 5% UVB (290–320 nm), is a major environmental risk factor for skin cancer, which afflicts more than 2 million people worldwide every year. UVB radiation can directly damage DNA, and thus is particularly carcinogenic. UVA can also cause cancer via the generation of DNA-damaging free radicals. Despite the harmful effects, UV-light exposure may have potential beneficial effects through the modulation of immune responses<sup>39</sup>. Indeed, UVB radiation can activate innate immune responses via release of antimicrobial peptides and vitamin-D production<sup>40,41</sup>, which may play a role in Finsen's phototherapy. UVB light also suppresses the adaptive immune system by activation of regulatory T cells, B cells and mast cells<sup>42</sup>.



UVA light can also be immunosuppressive through the upregulation of the alternative complement pathway<sup>43</sup>. These mechanistic findings have suggested a physiologic role for low, non-carcinogenic doses of UV light: induction of innate immunity to protect against microbial attacks, and suppression of adaptive immunity to inhibit autoimmune or allergic responses. The latter mechanism forms the basis of UV phototherapy, which is used to treat a wide range of dermatoses in the clinic<sup>44</sup>.

**Narrowband UVB therapy**—For over 90 years, UVB radiation has been used to treat psoriasis<sup>44,45</sup> — a chronic, immune-mediated inflammatory skin disorder affecting tens of millions of people worldwide. It is also used to treat vitiligo, atopic dermatitis and other inflammatory dermatoses. With emission at  $311\pm 2$  nm, narrowband UVB is preferable to standard broadband UVB (290–320 nm) because of improved efficacy and the reduced risk of erythema (superficial reddening of the skin).

**Psoralen and UVA therapy**—This is another frequent treatment for psoriasis and vitiligo. It requires oral or topical administration of psoralen and is commonly used to treat patients for whom narrowband UVB is unsuccessful<sup>46</sup>. The therapy also works through immunosuppressive and antiproliferative effects.

**Other effects**—Several epidemiology studies have noted that increased sun exposure is associated with decreased risk of multiple sclerosis<sup>47</sup>. A study in mice substantiated these findings, showing that UVB radiation suppresses the progression of experimental autoimmune encephalomyelitis<sup>48</sup>. Another mouse study suggested that UVB radiation may suppress the development of obesity and metabolic syndrome independent of vitamin-D supplementation<sup>49</sup>.

### Visible light (400–700 nm)

**Phototherapy for neonatal Jaundice**—Jaundiced infants are commonly treated with phototherapy at 460–490 nm, preventing serious sequelae of hyperbilirubinemia, such as permanent neurological damage<sup>38</sup> (Fig. 3e). Blue light isomerizes bilirubin to facilitate its excretion. In the United States, 0.5–4% of term and late-preterm infants receive phototherapy before discharge from the nursery. In low-resource settings, filtered sunlight using canopies is a promising and affordable option for treating neonatal jaundice<sup>50</sup>.

**Bright light therapy for mood disorders**—Seasonal affective disorder is a common form of depression that coincides with shorter days during the winter months and has a prevalence of 0.4–9.9% in the Northern Hemisphere<sup>51</sup>. This disorder and other conditions involving irregular light exposure, such as jet lag, have been linked to mood and cognitive alterations either by modulation of sleep and circadian rhythms, or by direct activation of neural pathways<sup>52</sup>. These mechanisms are mediated by intrinsically photosensitive retinal ganglion cells that express the photopigment melanopsin. Bright-light therapy has proven to be as effective as most antidepressant drugs for treating seasonal affective disorder<sup>53</sup>. In fact, activation of the ganglion cells by bright blue light (480 nm) conveys signals to the brain that suppress melatonin secretion and reset circadian rhythms<sup>54</sup>. Bright-light therapy has

also shown promise for the treatment of non-seasonal major depressive disorder<sup>55</sup>, but the mechanism of action is still unclear.

**Antimicrobial treatment**—Antibiotic resistance increasingly threatens the ability to effectively treat bacterial infections. Blue light at 405–470 nm has been effective in treating a broad range of bacterial infections, including *P. acnes*-associated acne vulgaris and *H. pylori* gastritis in humans, as well as wound infections with methicillin-resistant *S. aureus* (MRSA) and *P. aeruginosa* in mouse models<sup>56,57</sup>. The antimicrobial effect of blue light is thought to arise from the excitation of endogenous porphyrins within the bacterial cells. Before it is accepted for mainstream clinical practice, however, the possible development of microbial resistance to phototherapy needs to be evaluated.

**Other effects**—Insufficient outdoor exposure to sunlight has been implicated with the growing prevalence of myopia<sup>58</sup> (an estimated 2.5 billion people worldwide will be affected by the condition by 2020). Supporting this observation, high ambient lighting was found to prevent the development of myopia in macaque models<sup>59</sup>. Another potential application is the use of non-ablative lasers to adjuvant vaccines. Pre-treatment of the site of vaccine administration with visible or NIR light significantly enhanced vaccine efficiency and augmented immune responses in mouse models<sup>60</sup>.

#### Near-infrared light (700–1800 nm)

**Photobiomodulation**—Also known as low-level laser-light therapy (LLLT), photobiomodulation uses red and NIR light at 600–1000 nm, at fluences of 1–10 J/cm<sup>2</sup> with intensity of 3–90 mW/cm<sup>2</sup>. Clinical studies have suggested that light can stimulate epidermal stem cells in the hair follicle bulge to promote hair growth<sup>61</sup>. Photobiomodulation for wound healing, tissue repair and anti-inflammatory therapy<sup>62</sup> has been shown to be efficacious in animal models. Results from clinical trials have been mixed, yet have shown therapeutic potential for neck pain<sup>63</sup> and chronic traumatic brain injury<sup>64</sup>. Because its underlying mechanisms are not well understood, adoption of photobiomodulation has been controversial, and its use largely empirical. The mechanisms are largely attributed to the absorption of NIR light by cytochrome C oxidase in mitochondria. This triggers the dissociation of inhibitory nitric oxide from the protein complex, thus increasing ATP synthesis, which can have direct beneficial effects on compromised and hypoxic cells. Therapeutic effects of photobiomodulation may also be mediated by the generation of ROS and the induction of gene transcription. In fact, photobiomodulation on tooth pulps in rats with 810 nm cw light at a total dose of 3 J/cm<sup>2</sup> was shown to form tertiary dentin via direct dental stem cell differentiation through light-induced generation of ROS<sup>65</sup>.

**Thermal neuromodulation**—Optical modulation of neural or muscle activity is increasingly explored as a therapeutic option for neurological and cardiovascular diseases. Thermal neuromodulation by infrared light does not require any exogenous agents or genetic interventions<sup>66</sup>. The mechanism involves absorption of infrared light (1.8–2.2 μm) by water, producing a transient increase in temperature that alters the membrane capacitance and depolarizes the target cell. Pulsed laser light (for example, 0.25 ms and 1–2 J/cm<sup>2</sup>) has been used to stimulate and control heart beating in intact quail embryos<sup>67</sup> and cranial nerves for

nerve monitoring during surgery in gerbil models<sup>68</sup>, without causing apparent thermal damage. Although thermal neuromodulation lacks the precision and selectivity afforded by optogenetics, its non-invasive nature could make it more amenable to clinical translation.

### Photochemical crosslinking

Photoinduced crosslinking has a variety of applications in biomaterial engineering, biochip fabrication, drug synthesis and dental-composite curing. *In situ* polymerization of UV-epoxy is a common technique in the dental clinic. Corneal collagen crosslinking with riboflavin and UVA light (365 nm; 5 J/cm<sup>2</sup>) is a treatment for corneal ectasia, such as keratoconus<sup>69</sup> (crosslinking increases the stiffness of corneal stroma by 50–100%). Its application may expand to strengthening a corneal flap or to refractive error correction by beam shaping. Photochemical crosslinking could also be used to bond native collagen fibres to aid wound closure, and to enable the use of photopolymerizable biomaterials as surgical glue<sup>70,71</sup>. In tissue engineering, photopolymerization can be used to fabricate 3D tissue constructs<sup>72</sup>, or employed *in situ* to enable restoration of soft tissues<sup>73</sup>.

### Photodynamic therapy

Three components are required for PDT: a photosensitizer, light energy and oxygen. Following absorption of light by an exogenously delivered photosensitizer, energy is transferred from it to molecular oxygen, generating highly cytotoxic singlet oxygen and ROS. The efficacy of PDT is dependent on its ability to target diseased cells while sparing healthy cells, which requires selective accumulation of the photosensitizer and sufficient delivery of light energy to the target tissue. The antitumour effects of PDT result from the direct killing of tumour cells, the damage to tumour vasculature restricting oxygen and nutrient supply, and the induction of inflammatory responses that can result in systemic antitumour immunity<sup>74,75</sup>. Importantly, the mechanisms of cytotoxicity by PDT are fundamentally distinct from those of conventional chemotherapeutics; this may be leveraged in combinatorial therapies of PDT and chemotherapy in order to overcome resistance to cancer drugs<sup>76</sup>.

PDT is now clinically approved to treat a number of cancers, including those of the bladder, lung, skin, esophageal, brain, ovarian and bile duct<sup>75</sup> (Fig. 3f). In dermatology, PDT is commonly used for actinic keratosis and acne vulgaris, in addition to superficial non-melanoma skin cancers<sup>77</sup>. PDT is also approved to treat neovascular age-related macular degeneration, but its use has declined since the availability of anti-vascular-endothelial-growth-factor (anti-VEGF) therapy. Outside the clinic, PDT is used to eradicate viruses and other pathogens in blood products. For example, PDT with methylene blue is effective for inactivating viruses, including Hepatitis C, HIV-1 and West Nile, and since 1991 it has been used to treat over 4.4 million units of fresh frozen plasma in Europe<sup>78</sup>.

The poor penetration depth of light required for photosensitizer activation has limited clinical indications of PDT, which is currently only used for the treatment of superficial lesions, or of lesions accessible during surgery or through endoscopy. To extend the therapeutic depth, photosensitizers that can be activated with NIR light are under development<sup>75,79</sup>. Upconversion nanoparticles that convert incident NIR light to visible light

for indirect activation of conjugated photosensitizers have shown promise for treating deep-seated and solid tumours in animal models<sup>80</sup>. Another strategy is to deliver bioluminescent molecules directly to target tissues that are inaccessible by external illumination. For example, bioluminescent nanoparticles can activate photosensitizers via resonant energy transfer to treat lymph node metastases in mice<sup>81</sup>.

### Photothermal therapy

Since the early 1990s, hyperthermic therapy using externally applied radiofrequency, microwave or ultrasound to heat tumours has been used as an adjunct to chemotherapy and radiotherapy to enhance treatment response<sup>82</sup>. In more recent years, the use of thermal agents such as magnetic nanoparticles to selectively localize heat to target tumour cells has shown considerable potential (photothermal therapy can be effective for treating hypoxic tumours, as it does not require oxygen<sup>83</sup>). Strongly absorbing nanoparticles, such as gold nanocages, can induce hyperthermia or thermal ablation. Among NIR-absorbing noble metal nanoparticles utilizing surface plasmon resonances<sup>84</sup>, only gold nanoshells have been tested in patients (in on-going clinical trials for lung and head-and-neck tumours). In fact, the clinical translation of these biodegradable inorganic nanoparticles has been slowed by concerns over their biocompatibility, clearance and long-term toxicity. This has spurred the development of biodegradable organic photothermal agents<sup>85</sup>, such as porphyrin nanoparticles<sup>86</sup>.

### Optical diagnostics and imaging

Optical technologies are used along the entire spectrum of diagnostic medicine, from point-of-care and laboratory testing, to screening and diagnostic imaging, to treatment monitoring, to intraoperative imaging. Optical imaging enables real-time visualization of tissues and cells at high spatial resolutions with instrumentation that is relatively inexpensive and portable, especially compared to MRI and CT. A variety of macroscopic and microscopic imaging technologies have been adopted in clinical practice as standard of care, are currently in clinical adoption phases, or are under development for clinical translation (Fig. 4). In the operating room, surgical techniques that rely on optical guidance, such as laparoscopic surgery, have reduced the risk of haemorrhage and shortened patient recovery time. Intraoperative optical imaging provides tissue contrast beyond what can be perceived by the human eye, resulting in improved surgical outcomes. In this section, we discuss optical technologies that have enhanced the physician's ability to screen for, diagnose and monitor disease, with a focus on applications that have addressed previously unmet clinical needs.

### Point-of-care testing

Optical technologies are an integral part of patient care, from routine physical examinations to bedside diagnostic testing. Relatively simple instruments such as the otoscope<sup>87</sup> and the ophthalmoscope enhance visual inspection of tissues. Probing light absorption and scattering by tissue constituents enables measurement of important diagnostic indicators, including haemodynamics and the presence of specific biomarkers. The most prominent example is the pulse oximeter, which relies on absorption differences between oxygenated and deoxygenated haemoglobin to estimate the patient's arterial oxygen saturation. Beyond its

universal use in emergency medicine, pulse oximetry has also become an effective screening tool for congenital heart defects in newborns<sup>88</sup>. NIR spectroscopy, also relying on haemoglobin absorption, is an emerging tool for non-invasive monitoring of brain function<sup>89</sup>. Spectroscopic techniques sensitive to changes in cellular chromophore concentrations are also being developed for cancer screening, such as for the diagnosis of oral cancer<sup>90</sup>. Dynamic light scattering techniques are increasingly adopted in the clinic for rapid, real-time assessment of microvascular function<sup>91</sup>, such as for burn wounds or atherosclerosis. Two techniques relying on NIR-laser light scattered by moving red blood cells are laser Doppler imaging, which detects frequency-shifted light, and laser speckle contrast imaging<sup>92</sup>, which measures motion-induced intensity fluctuations.

Extensive efforts have been made in the development of optical technologies for point-of-care testing in resource-limited settings<sup>93</sup>. Lens-free computational imaging has eliminated the need for costly optical components, enabling the development of low-cost, portable, on-chip diagnostic platforms<sup>94</sup>. Ubiquitous optical devices such as smartphone cameras may be modified to add diagnostic functionalities such as calorimetric detection<sup>95</sup>, multiplexed detection<sup>96</sup>, video microscopy<sup>97</sup> and high-resolution spectroscopy<sup>98</sup>. With the continued development of optical technologies, such as fibre optics, optoelectronics and optical microelectromechanical systems, various optical-imaging platforms may be miniaturized for widespread use in point-of-care settings<sup>99</sup>.

### Molecular diagnostics

Optical techniques have been a mainstay of pathology analysis in the laboratory for over a century. For example, light microscopy is routinely used to analyse peripheral blood smears for haematologic disorders. Flow cytometry, typically through fluorescence-activated cell sorting (FACS), is commonly used for molecular phenotyping of haematologic malignancies and immune disorders, as well as for purifying cellular subpopulations for cell-based therapies. The enzyme-linked immunosorbent assay (ELISA), in which a colour change indicates the binding of specific proteins, is the gold standard for detection of serum antibodies and various biomarkers of disease. To improve sensitivity of protein detection, a number of optical approaches have been proposed, including surface plasmon resonance<sup>100</sup>, surface enhanced Raman scattering<sup>101</sup> and resonant optical cavity sensing<sup>102,103</sup>. Recent innovations in genetic sequencing have ushered in a new era of precision medicine, in which treatment regimens are tailored to patient genotypes. Optical probes are integral tools in genetic analyses, including fluorescence *in situ* hybridization, DNA microarrays and high-throughput sequencing. Future diagnostic tools are likely to combine both optical imaging and sequencing capabilities to fully capture the genetic and phenotypic complexity needed to treat heterogeneous diseases such as cancer<sup>104,105</sup>.

### Diagnostic imaging

With its non-invasiveness, high-resolution, and rich contrast mechanisms, optical imaging is an established and rapidly growing modality for screening and diagnosis. In what follows, we briefly discuss the most relevant optical-imaging methods.

**Endoscopy**—The standard white-light endoscope is one of the most basic yet essential optical instruments used by physicians to examine the inner organs of patients, such as the gastrointestinal and respiratory tracts<sup>106</sup>. Improvements in optical technologies have greatly enhanced the capabilities of endoscopic imaging, which has coincided with the rapid growth of the endoscopy equipment market (Fig. 2d), projected to reach \$38 billion by 2018 (Markets and Markets). Chromoendoscopy uses dyes or stains to aid tissue characterization, such as dysplastic mucosa<sup>107</sup>. Narrow band imaging, which does not require dyes, relies on the light-penetration difference between blue and green light (typically, 415 and 540 nm) to enhance the visibility of superficial and deeper blood vessels.

**Capsule endoscopy**—Over the past decade, wireless video capsule endoscopy has become an increasingly popular non-invasive tool for the diagnosis of small bowel disorders<sup>108</sup>. Approved capsule endoscopes consist of a camera sensor, a light-emitting-diode light source, a battery, and a wireless radiofrequency transmitter. The capsule is swallowed with water, and excreted with bowel movements. Capsule endoscopes are often the treatment of choice for obscure gastrointestinal bleeding in adults, as they enable the examination of the entire length of the small bowel<sup>109</sup>. They are used increasingly for the assessment of Crohn's disease and for the detection of small bowel tumours.

**Ophthalmic imaging**—A variety of optical instruments are routinely employed to examine a patient's vision. For example, the slit lamp is used to visualize the anterior and posterior segments of the eye. Rotating the slit illumination in conjunction with a Scheimpflug camera allows for the measurement of corneal topography and of intraocular pressure by analysing corneal deformation in response to air puff. Other commonly used instruments include wavefront sensors, confocal ophthalmoscopes and fundus cameras. Optical coherence tomography (OCT) is used to obtain high-resolution images of corneal and retina morphology. OCT is the standard of care for diagnosis of pathologies such as glaucoma and age-related macular degeneration<sup>110</sup>. OCT imaging of retinal anatomy is also being explored as a marker for neurological disorders, including multiple sclerosis and Alzheimer's.

**Optical coherence tomography**—OCT is an established modality for high-resolution, label-free, non-invasive imaging<sup>111</sup>. The global market for OCT equipment is growing, and is expected to reach \$1.4 billion by 2019. OCT provides cross-sectional images of tissue microstructure by measuring the echo time delay and intensity of backscattered light at different depths (up to 2–3 mm) at a resolution of 3–15  $\mu\text{m}$ , typically using a broadband light source (800–900 nm) or a wavelength-swept laser (1200–1400 nm)<sup>112</sup>. Beyond ophthalmic applications, OCT is clinically approved for catheter-based intracoronary imaging<sup>113</sup>, and has been used for the monitoring of outcomes of intracoronary stenting, for assessing coronary plaques in the management of patients with acute coronary syndrome, and for the accurate quantification of thin fibrous cap thickness as a marker of plaque vulnerability<sup>114</sup>. Another target for OCT is endoscopic imaging of the upper gastrointestinal tract<sup>115</sup>. Technical innovations that may improve the diagnostic capabilities of OCT include cellular resolution<sup>116</sup>, angiography, high-frame rates, birefringence measurement and multimodality<sup>117</sup>.



**Diffuse optical tomography**—Diffuse optical spectroscopic tomography (DOT) is a label-free method that uses NIR light to probe tissue concentrations of haemoglobins, water and lipids. It has been successful in monitoring the response to neoadjuvant chemotherapy in breast-cancer patients<sup>118,119</sup>. Non-responders and responders could be differentiated as early as the first day after chemotherapy, which would allow non-responders to change treatment strategies early, thus avoiding unnecessary toxicities from additional chemotherapy. The chromophore signatures obtained by DOT can also be used to predict the response to neoadjuvant chemotherapy in breast-cancer patients prior to treatment<sup>120</sup>. DOT combined with X-ray mammography has shown potential in reducing the false-positive rate of conventional mammography<sup>121</sup>. Recent DOT technology has also enabled functional neuroimaging of the superficial cortex, with images of quality similar to those from functional MRI (fMRI)<sup>122</sup>. DOT could thus be advantageous for patients with MRI-incompatible implants or for neonates in intensive care<sup>123</sup>.

**Fluorescence imaging**—Confocal laser endomicroscopy (CLE)<sup>124</sup> uses fluorescence contrast and fibre-bundle probes to generate high-magnification images of the gastrointestinal mucosa. Confocal detection, or collection of fluorescence light only from the illuminated focal plane, enhances spatial resolution compared to conventional endoscopy, enabling assessment of mucosal histology. CLE has shown promise in the detection of neoplasia in patients with Barrett's oesophagus, as well as improved sensitivity over chromoendoscopy in the classification of colorectal polyps<sup>125</sup>, in the assessment of inflammation bowel disease<sup>126</sup>, and in the diagnosis of bladder cancer<sup>127</sup>. For molecular imaging, fluorescently labelled peptides that specifically bind to dysplastic tissue have been used to detect colonic dysplasia<sup>128</sup> and esophageal neoplasia<sup>129</sup>. Fluorescent lectins that bind to normal tissue can also be used as negative contrast agents<sup>130</sup>. Although the high resolution of confocal laser endomicroscopy enables accurate image quantification, it is limited by the small field of view, which precludes efficient examination of large areas to detect lesions. This has driven the development of molecular imaging with wide-field fluorescence endoscopy. For example, blue-light cystoscopy with fluorescent labelled CD47 antibodies enabled the detection of bladder cancer in *ex vivo* specimens<sup>131</sup>, and neoplastic colorectal polyps in humans were detected through fluorescent peptides targeting c-Met<sup>132</sup>. Recently, fluorescence angiography has been used to visualize tissue perfusion in extremity wounds, such as diabetic foot ulcers<sup>133</sup>. Continued development of molecular imaging agents and optical technologies will likely fulfil the promise of characterizing lesions *in vivo*, improving diagnostic accuracy and reducing pathology costs.

**Nonlinear microscopies**—Two-photon microscopy offers the benefit of deeply penetrating NIR light as well as light absorption confined to the focal plane, improving optical sectioning in tissue. However, its use has generally been limited to tissue specimens and small-animal imaging<sup>134</sup>, due to the requirement of a femtosecond laser with high peak power. Nonetheless, two-photon microscopy has been used for the diagnosis of malignant melanoma in humans through the imaging of endogenous chromophores<sup>135</sup>. Another target is the non-invasive imaging of retinal pigment epithelium, in particular retinosomes containing fluorescent metabolic products associated with age-related macular degeneration<sup>136</sup>. Nonlinear Raman scattering techniques enable label-free imaging of

intrinsic molecular vibrations, generating optical contrast between lipids and proteins<sup>137</sup>. Stimulated Raman scattering microscopy was used to detect brain-tumour infiltration in fresh specimens from neurosurgical patients, demonstrating near-perfect agreement with standard haematoxylin and eosin light microscopy<sup>138</sup>.

**Photoacoustic imaging**—Photoacoustic or optoacoustic imaging relies on the photoacoustic effect, in which absorption of a periodic train of nanosecond laser pulses induces cyclic, localized heating and cooling, generating pressure waves that can be detected by ultrasound transducers<sup>139</sup>. Its major advantages include enhanced depth penetration compared to optical imaging, and multispectral imaging of multiple endogenous or exogenous absorbers. This technique can be readily integrated with commercial ultrasound probes to enhance image contrast through the detection of vasculature or contrast agents<sup>140</sup>. The sensitivity can also be leveraged for the *in vivo* detection of circulating tumour cells in rodent models<sup>141</sup>. In initial patient studies of breast-cancer imaging, it has shown promise for the imaging of tumour vasculature and oxygenation with higher spatial resolution than DOT<sup>142,143</sup>.

**Other techniques**—Reflectance confocal microscopy is an accurate non-invasive technique for the diagnosis of basal cell carcinoma<sup>144</sup>, and may be able to diagnose melanoma<sup>145</sup>. Brillouin microscopy relies on light scattering from spontaneous acoustic waves in tissue to provide biomechanical information of transparent ocular tissues. It has been used in humans *in vivo* to map stiffness in healthy and keratoconus corneas<sup>146</sup>.

### Imaging in surgery and therapy

Optical imaging during surgical operation has become increasingly indispensable, guiding the surgeon's eye through narrow endoscopic channels, and providing greater contrast and higher resolution between healthy and disease tissues than perceived by the naked eye.

**Endoscopic imaging**—Minimally invasive surgeries, or endoscopic surgeries, have dramatically changed the way operations are performed. In the United States, 96% of cholecystectomies are performed with laparoscopy<sup>147</sup>, whereas many other procedures increasingly use minimally invasive techniques<sup>148</sup>. Compared to open procedures, laparoscopic techniques have resulted in superior surgical outcomes due to smaller scars, fewer complications and quicker recovery. Advances in optical devices and technologies have enabled surgeons to operate effectively without direct visualization of the target tissue. Stereoscopic vision has been employed in precision robotic surgery<sup>149</sup>.

**Intraoperative imaging**—For open-field procedures, surgeons rely on visual inspection and palpation to differentiate between healthy and diseased tissue. However, human vision through white-light reflectance cannot easily discriminate between different tissue types, and is limited by haemoglobin absorption and tissue scattering. For cancer surgeries, the ability to discriminate between malignant and normal tissue is paramount for determining which tissues to resect or preserve. A growing number of clinical trials in recent years have showcased the promise of fluorescence-guided surgery in improving surgical outcomes, decreasing surgical time and lowering overall healthcare costs<sup>150,151</sup>.

Fluorescence-guided surgery has been adopted for the resection of high-grade gliomas<sup>152</sup>. Orally administered 5-aminolevulinic acid (ALA) is metabolically activated to form protoporphyrin IX, which accumulates in tumour tissues and exhibits red fluorescence. A phase-III trial showed significantly improved complete resection and survival when ALA guidance was used rather than white-light illumination<sup>153</sup>. Similarly, ALA has been used to guide tumour resection of bladder cancer, resulting in improved outcomes.

Exogenous NIR fluorescent probes are ideal for intraoperative imaging because of minimal background autofluorescence and enhanced tissue penetration over visible light. Currently, the only NIR probe approved by the Food and Drug Administration and the European Medicines Agency is indocyanine green (ICG)<sup>151</sup>. Other probes with reduced background<sup>154</sup> and high tissue specificity<sup>155</sup> are under development. The clinical utility of ICG for surgical guidance has been demonstrated for the mapping of sentinel lymph nodes<sup>156</sup> and in the detection of previously undetectable small liver metastases<sup>157</sup>.

**Molecular imaging**—The next frontier for fluorescence-guided surgery involves molecular targeted contrast agents. In 2011, the first in-human trial of tumour-specific fluorescence-guided surgery was conducted in patients with ovarian cancer<sup>158</sup>. Using folate-fluorescein-isothiocyanate to target folate-receptor- $\alpha$ , which is expressed in 90–95% of patients with epithelial ovarian cancer, surgeons were able to identify significantly more tumour deposits than with visual inspection alone. However, folate-receptor- $\alpha$  is overexpressed only in certain cancers, which limits the general applicability of folate-conjugated dyes. Another approach currently in development uses activatable probes that become fluorescent when exposed to proteases overexpressed in tumours, thus enabling optical contrast between normal and tumour tissues<sup>159–162</sup>. Labelling peripheral nerves with fluorescent peptides may also prevent accidental transection of nerves during surgery<sup>160</sup>.

**Microscopic and spectroscopic guidance**—Although large-field-of-view, fluorescence-based imaging is most suited for surgical guidance in the operating room, optical microscopy techniques with high resolution and reduced field of view have also demonstrated intraoperative utility. OCT has been widely used for ophthalmologic surgeries<sup>163</sup>, and in conjunction with angiography for percutaneous coronary intervention<sup>164</sup>. OCT and stimulated Raman scattering microscopy have been shown to delineate brain tumours in mice *in vivo*<sup>165,166</sup>. Raman scattering spectroscopy was used to detect brain cancer cells in humans during brain surgery<sup>167</sup>. Rapid detection of cancer cells by optical methods could therefore become an invaluable tool for surgical decision-making.

**Optical imaging in theranostics**—Broadly defined, theranostics refers to the combination of therapeutic modalities and diagnostic imaging to adjust treatment protocols to the needs of individual patients. Optical imaging can facilitate the detection of pathologies, the determination of target location and dosimetry, and the monitoring of therapeutic effects *in situ*. Optical imaging is particularly well-suited for guiding light-activated therapies, which require light sources. Detection of photosensitizer fluorescence is commonly used for the monitoring and optimization of photodynamic therapy<sup>168,169</sup>. *In vivo* fluorescence molecular imaging can also be used to predict therapeutic outcomes, as has

been shown for cancer<sup>170</sup> and Crohn's disease<sup>171</sup>. And optical Cherenkov emission from radioisotopes could be useful for the dosimetry of X-ray external-beam radiation therapy<sup>172</sup>.

## Emerging technologies

With the success of medical lasers and optical technologies and the recognition of the needs and opportunities for better healthcare (Table 1), considerable efforts have been made to develop improved or new light-based technologies. Technological innovations continue to push the envelope of optical imaging, including super-resolution imaging beyond the diffraction limit<sup>173</sup>, and rapid 3D imaging with light-sheet microscopy<sup>174</sup>. Tissue-clearing techniques that render entire organs optically transparent while preserving tissue microstructure<sup>175</sup> may enhance clinical histologic evaluation. Spatial light modulation that counteracts scattering in tissues for improved light penetration and resolution could lead to practical tools for imaging, endoscopy and light-activated therapies<sup>176</sup>. Besides advances in optics and photonics, progress in other fields, such as nanotechnology, bio-inspired engineering, genome editing, and advanced materials have opened up opportunities for further innovation in photomedicine. Injectable multifunctional nanoparticles enable light energy to be relayed to specific cells of interest while providing spatiotemporal control of light activation. Genetic integration of fluorescent proteins enables the identification of molecular targets, whereas optogenetics offers precise control of cellular function in the nervous system. These technologies harness the molecular specificity of light-tissue interactions to meet the need for more precise and personalized therapies, such as the targeting of vulnerable cancer cells identified by molecular profiling. At the same time, advances in biomaterials and optoelectronics have led to novel optical devices that are wearable or safely integrated into the human body, allowing continuous health monitoring and providing new opportunities to deliver light to targets previously inaccessible by external illumination.

### Light-activated nanomedicine

Nanoparticles based on lipid, polymeric and inorganic materials have advantages over molecular-based therapeutics, such as tunability of size and shape, versatile functionalization capabilities for active targeting, and unique optical properties<sup>177</sup>. Light-triggered drug release from nanoparticles enables the on-demand, spatiotemporally controlled delivery of therapeutic agents. This allows dosing regimens to be tailored to patient needs while increasing drug concentration at target tissues and reducing systemic toxicities. For cancer patients, the optimal timing of chemotherapeutic treatment could enhance antitumor efficacy and reduce metastatic spread<sup>178</sup>. Strategies for nanoparticle-mediated drug delivery include transduction by upconversion nanoparticles<sup>179</sup>, NIR-light induced heating of thermosensitive polymers<sup>180</sup> (Fig. 5a), and permeabilization of drug-containing liposomes<sup>181</sup>.

Multifunctional nanoparticles that bear a combination of diagnostic and therapeutic functionalities —theranostic agents — are of particular interest for precision medicine, as they combine both biomarker identification and therapy in a single platform. Theranostic capabilities can span a wide array of modalities, including fluorescence and photoacoustic imaging, PET, MRI, photodynamic and photothermal therapy, and drug delivery<sup>182–186</sup>. The

spatiotemporal localization and synchronization of these multimodal therapies can lead to synergistically enhanced therapeutic efficacy. One promising approach is the nanoparticle-mediated combination of PDT and chemotherapy<sup>187,188</sup> (Fig. 5a). Another example takes advantage of clustering of drug-loaded liposomes and antibody-targeted gold nanoparticles inside cancer cells<sup>189</sup>. When exposed to laser light, a plasmonic nanobubble destroys the host cancer cell, ejecting chemotherapeutic drugs and potentiating the effects of X-ray radiation therapy.

A major barrier to systemically administered nanomedicines, particularly for cancer therapy, is the inefficient delivery of nanoparticles to the tumour or target site<sup>190</sup>. Overcoming this barrier will require both improvements in nanoparticle design and better understanding of biological responses to nanoparticle delivery<sup>191</sup>. In future, applications of light-activated nanoparticles are likely to extend beyond imaging and the delivery of direct therapeutic payloads<sup>192</sup>. Indeed, light activation may be useful for modulating biological behaviours at the systems level for therapeutic benefit; for example, NIR-light-induced heating of gold nanorods has been used to cause a clotting cascade in tumours, which then amplified the delivery of chemotherapeutics targeted to a by-product of the coagulation cascade<sup>193</sup>. Another potential avenue is the manipulation of nanorobots to perform complex tasks *in vivo* (such as precise, non-invasive surgeries). Towards this end, a recently developed light-controlled, programmable artificial microswimmer sensed and oriented its migration to the direction of external illumination<sup>194</sup> (Fig. 5b).

### Optogenetic therapies

Optogenetics has revolutionized the way light can be used to control cellular activity<sup>195</sup>. In a typical protocol, target cells are rendered photoactive via genetic integration of microbial opsins (light-gated ion channels), thus enabling optical control of electrical activity. Optogenetic techniques have enabled unprecedented insights into disease circuitry, which led to immediate clinical impact. For example, optical dissection of brain circuitry in mouse models revealed mechanisms of deep brain stimulation in the treatment of Parkinson's disease<sup>196</sup>, and helped to design new deep-brain-stimulation protocols for treating cocaine addiction<sup>197</sup>.

Because of its capabilities for neuromodulation therapy, optogenetics has enticing clinical potential. However, significant barriers to human use remain, such as the need for genetic transfection and proper illumination<sup>198,199</sup>. Optogenetic therapy for conditions such as depression<sup>200</sup>, chronic pain<sup>201</sup> and laryngeal paralysis<sup>202</sup> has been tested in rodent models and may one day be translated for human use. Orphan status was recently granted to a viral-vector-based optogenetic therapy (from RetroSense Therapeutics) for retinitis pigmentosa, thus paving the way for future clinical trials. In this case, optogenetic transfection can impart light-sensing ability to relevant cell types (such as ON-bipolar cells) located downstream of the damaged photoreceptors<sup>203</sup>. A more recent concept is the coupling of an optogenetic retinal prosthesis with a high-radiance optical-stimulation display device<sup>204</sup> (Fig. 5c).

A long-term limitation of optogenetic therapies concerns the potential adverse immune responses resulting from the xenotransplantation of microbial proteins into humans. Light-activated control of native ion channels can also be achieved through exogenously delivered

caged molecules or photoswitchable compounds<sup>205</sup>. Indeed, photoisomerizable photoswitches have been used to restore visual responses in blind mice<sup>206</sup>, and to reversibly control nociception in rats<sup>207</sup>. To enable genetic targeting to specific cells, mammalian ion channels can be engineered to impart light-gated functionality<sup>208</sup>, enabling restoration of retinal function in blind mice and dogs<sup>209</sup>. Melanopsin — a mammalian opsin that controls G-protein-signalling pathways — can also be introduced to render cells photosensitive<sup>210</sup>. These optogenetic tools can create synthetic gene circuits with therapeutic applications. For example, an optogenetic circuit that regulates the expression of glucagon-like peptide-1 was developed for the treatment of type 2 diabetes. When implanted in diabetic mice, the engineered optogenetic cells improved blood-glucose homeostasis upon treatment with blue light<sup>211,212</sup>. Therapies involving the implantation of genetically modified cells rather than *in vivo* gene therapy could have an easier path to clinical translation.

### Wearable, personal healthcare devices

The skin offers a promising site for measuring physiological information (such as body temperature) for continuous health monitoring<sup>213</sup> (Fig. 5d). The development of low-cost, stretchable and flexible optoelectronics<sup>214,215</sup>, such as polymer LEDs, may enable a range of wearable health-monitoring devices in both clinical and at-home settings. Examples include a flexible, all-organic optoelectronic pulse oximeter that has comparable efficiency to commercially available oximeters<sup>216</sup>, and a wireless, stretchable optoelectronics device worn on the skin for monitoring blood flow<sup>217</sup> (Fig. 5d). Future wearable devices could incorporate therapeutic functionalities, such as antibacterial blue-light therapy or low-level light therapy. Flexible optoelectronic devices may also be incorporated into endoscopes for multimodal theranostic functionality<sup>218</sup> (Fig. 5e).

### Implantable optoelectronic devices

A significant portion of the over-\$200-billion-per-year global medical device market is for devices that are implanted in the human body. Artificial intraocular lenses make the largest number of implanted medical devices, accounting for nearly 40% of the market in 2011. Prosthetic retinas promise to restore vision in patients blinded by the degeneration of retinal photoreceptor cells, and their development is being fuelled by advances in optoelectronic technologies (Fig. 5f)<sup>219</sup>. With rapid advances in bio-optic interface technologies and heightened recognition of light versatility in diagnostics and therapies, many new implantable devices based on light-based functionalities are likely to emerge. Novel device concepts and designs include implantable light emitting diodes<sup>220</sup>, miniaturized wireless optoelectronic devices for optogenetic applications<sup>221–223</sup>, and optofluidic controlled drug delivery<sup>224</sup> (Fig. 5e). Remotely powered, wireless LED implants offer the potential to enable light-activated therapies in the body. Using radiofrequency<sup>225</sup> or mid-field transmission<sup>226</sup>, it is possible to transfer a few mW of electrical power over 10 cm across tissue, sufficient to drive an LED or laser diode for optical sensing and chronic PDT (Fig. 5g). Besides battery or wireless powering, these devices may be self-powered by harnessing kinetic energy from muscular movements<sup>227</sup>. LEDs may also be integrated into existing device platforms, such as gastrointestinal stents<sup>228</sup>.



## Biomaterial photonic devices

To fully realize the diversity in light–tissue interactions for medical applications, light must be delivered to target tissues with sufficient energy and specificity. Biomaterial waveguides may be used for long-term light delivery<sup>229</sup> and need not be removed if made of biodegradable materials, such as silk or absorbable sutures made of polyglycolic acid<sup>230</sup> (Fig. 5h). Light-controlled therapy and sensing have been demonstrated by using fibre-optic hydrogel implants with fluorescent reporters and optogenetic cells<sup>212</sup> (Fig. 5h). Multifunctional optical fibres may be implanted for neuromodulation of the nervous system in the body<sup>231</sup>. Cell-based lasers may offer new ways of delivering light by exploiting the intrinsic capabilities of the cells carrying intracellular lasers<sup>232</sup> (Fig. 5i) to target, for example, sites of inflammation, and to permit highly-multiplexed imaging based on narrowband coherent emission<sup>233</sup>.

## Outlook

Laser surgery and treatments, particularly in dermatology and ophthalmology, are clinically established yet steadily growing areas. Development of new, compact and cost-effective lasers delivering desired output characteristics will expand clinical utilities and enhance treatment outcomes. Phototherapies and photoactivated drug therapies have a long history, yet only a handful of modalities have been adopted as first-line treatments in modern medicine. Yet recent progress in the understanding of light–tissue interactions, drug delivery and nanotechnologies will accelerate clinical translation. Optical diagnostics and imaging have enjoyed growing clinical adoption in many areas and will find increasing utilities. The wide variety of strategies for enhancing imaging contrast, resolution and molecular specificity make optical imaging a powerful modality, along with those of conventional radiologic imaging. Given the versatile role of light in nature, the many ways that light-based approaches can sense, monitor and manipulate biological processes is not surprising. In years to come, increased integration of light-sensitive functionalities in patients through genetic engineering, implantable optoelectronics, and intracellular devices such as micro- and nanolasers, will further enrich the role of light in medicine. As noted in 1909 by the radiographer Harvey van Allen<sup>234</sup>, “Many other things have been claimed for light treatment, but other methods have proved better in those cases in my hands. We need to look at these things carefully and not be carried away by our enthusiasm.” More than a century later, the excitement in photomedicine is still high.

## Acknowledgments

This work was supported by the U.S. National Institutes of Health grants DP1-OD022296, P41-EB015903, R01-EY025454, R01-CA192878 and National Science Foundation grants ECCS-1505569, CMMI-1562863.

## References

1. Zaret MM, et al. Ocular lesions produced by an optical maser (laser). *Science*. 1961; 134:1525–1526. [PubMed: 14009883]
2. Goldman L, Wilson RG. Treatment of basal cell epithelioma by laser radiation. *JAMA*. 1964; 189:773–775. [PubMed: 14174061]

3. Sakimoto T, Rosenblatt MI, Azar DT. Laser eye surgery for refractive errors. *Lancet*. 2006; 367:1432–1447. [PubMed: 16650653]
4. Marshall J, Trokel S, Rothery S, Krueger R. Long-term healing of the central cornea after photorefractive keratectomy using an excimer laser. *Ophthalmology*. 1988; 95:1411–1421.
5. Solomon KD, et al. LASIK world literature review: quality of life and patient satisfaction. *Ophthalmology*. 2009; 116:691–701. [PubMed: 19344821]
6. Palanker DV, et al. Femtosecond laser-assisted cataract surgery with integrated optical coherence tomography. *Sci Transl Med*. 2010; 2:58ra85.
7. Karabag RY. Retinal tears and rhegmatogenous retinal detachment after intravitreal injections: its prevalence and case reports. *Digit J Ophthalmol*. 2015; 21:8–10. [PubMed: 27330458]
8. Sternberg P. Subfoveal neovascular lesions in age-related macular degeneration. Guidelines for evaluation and treatment in the macular photocoagulation study. *Arch Ophthalmol*. 1991; 109:1242–1257. [PubMed: 1718252]
9. Tanzi EL, Lupton JR, Alster TS. Lasers in dermatology: four decades of progress. *J Am Acad Dermatol*. 2003; 49:1–34. [PubMed: 12833005]
10. Anderson RR, Parrish JA. Selective photothermolysis: precise microsurgery by selective absorption of pulsed radiation. *Science*. 1983; 220:524–527. [PubMed: 6836297]
11. Anderson RR, Parrish Ja. Microvasculature can be selectively damaged using dye lasers: a basic theory and experimental evidence in human skin. *Lasers Surg Med*. 1981; 1:263–276. [PubMed: 7341895]
12. Nelson JS, et al. Dynamic epidermal cooling during pulsed laser treatment of port-wine stain. A new methodology with preliminary clinical evaluation. *Arch Dermatol*. 1995; 131:695–700. [PubMed: 7778922]
13. Fitzpatrick RE, Goldman MP, Satur NM, Tope WD. Pulsed carbon dioxide laser resurfacing of photo-aged facial skin. *Arch Dermatol*. 1996; 132:395–402. [PubMed: 8629842]
14. Manstein D, Herron GS, Sink RK, Tanner H, Anderson RR. Fractional photothermolysis: a new concept for cutaneous remodeling using microscopic patterns of thermal injury. *Lasers Surg Med*. 2004; 34:426–438. [PubMed: 15216537]
15. Sherling M, et al. Consensus recommendations on the use of an erbium-doped 1,550-nm fractionated laser and its applications in dermatologic laser surgery. *Dermatologic Surg*. 2010; 36:461–469.
16. Kositratna G, Evers M, Sajjadi A, Manstein D. Rapid fibrin plug formation within cutaneous ablative fractional CO<sub>2</sub> laser lesions. *Lasers Surg Med*. 2016; 48:125–132. [PubMed: 26388136]
17. Kilmer SL, Anderson RR. Clinical use of the Q-switched Ruby and the Q-switched Nd:YAG (1064 nm and 532 nm) lasers for treatment of tattoos. *J Dermatol Surg Oncol*. 1993; 19:330–338. [PubMed: 8478472]
18. Reddy KK. Successful and Rapid Treatment of Blue and Green Tattoo Pigment With a Novel Picosecond Laser<alt-title>Picosecond Laser Treatment of Blue, Green Tattoo</alt-title>. *Arch Dermatol*. 2012; 148:820. [PubMed: 22801616]
19. Grossman MC, Dierickx C, Farinelli W, Flotte T, Anderson RR. Damage to hair follicles by normal-mode ruby laser pulses. *J Am Acad Dermatol*. 1996; 35:889–894. [PubMed: 8959946]
20. Metelitsa AI, Green JB. Home-use laser and light devices for the skin—an update. *Semin Cutan Med Surg*. 2011; 30:144–147. [PubMed: 21925367]
21. Jackson SD. Towards high-power mid-infrared emission from a fibre laser. *Nat Photonics*. 2012; 6:423–431.
22. Gillling P, Cass C, Cresswell M, Fraundorfer M. Holmium laser resection of the prostate: preliminary results of a new method for the treatment of benign prostatic hyperplasia. *Urology*. 1996; 47:48–51. [PubMed: 8560662]
23. Malek RS, Kuntzman RS, Barrett DM. High-power potassium-titanyl-phosphate (KTP/532) laser vaporization prostatectomy: 24 hours later. *Urology*. 1998; 51:254–256. [PubMed: 9495707]
24. Sofer M, et al. Holmium:YAG laser lithotripsy for upper urinary tract calculi in 598 patients. *J Urol*. 2002; 167:31–34. [PubMed: 11743269]

25. Ell C, Lux G, Hochberger J, Müller D, Demling L. Laserlithotripsy of common bile duct stones. *Gut*. 1988; 29:746–751. [PubMed: 2898421]
26. Wazni O, et al. Lead extraction in the contemporary setting: the LEXIcon study: an observational Retrospective study of consecutive laser lead extractions. *J Am Coll Cardiol*. 2010; 55:579–586. [PubMed: 20152562]
27. Wilkoff BL, et al. Pacemaker lead extraction with the laser sheath: results of the pacing lead extraction with the excimer sheath (PLEXES) trial. *J Am Coll Cardiol*. 1999; 33:1671–1676. [PubMed: 10334441]
28. Grundfest WS, et al. Laser ablation of human atherosclerotic plaque without adjacent tissue injury. *J Am Coll Cardiol*. 1985; 5:929–933. [PubMed: 3838324]
29. Min RJ, Khilnani N, Zimmet SE. Endovenous laser treatment of saphenous vein reflux: long-term results. *J Vasc Interv Radiol*. 2003; 14:991–996. [PubMed: 12902556]
30. Proebstle TM, Moehler T, Herdemann S. Reduced recanalization rates of the great saphenous vein after endovenous laser treatment with increased energy dosing: Definition of a threshold for the endovenous fluence equivalent. *J Vasc Surg*. 2006; 44:834–839. [PubMed: 16945499]
31. Mccoppin HH, Hovenic WW, Wheeland RG. Laser treatment of superficial leg veins. *Dermatologic Surg*. 2011; 37:729–741.
32. Hibst R, Keller U. Experimental studies of the application of the Er:YAG laser on dental hard substances: I. Measurement of the ablation rate. *Lasers Surg Med*. 1989; 9:338–344. [PubMed: 2761329]
33. Wigdor HA, et al. Lasers in dentistry. *Lasers Surg Med*. 1995; 16:103–133. [PubMed: 7769957]
34. Strong MS, Jako GJ. Laser surgery in the larynx - Early clinical experience with continuous CO<sub>2</sub>-laser. *Ann Otol Rhinol Laryngol*. 1972; 81:792–798.
35. Amin Z, et al. Hepatic metastases: interstitial laser photocoagulation with real-time US monitoring and dynamic CT evaluation of treatment. *Radiology*. 1993; 187:339–347. [PubMed: 8475270]
36. Mellow MH, Pinkas H. Endoscopic laser therapy for malignancies affecting the esophagus and gastroesophageal junction: Analysis of technical and functional efficacy. *Arch Intern Med*. 1985; 145:1443–1446. [PubMed: 4026476]
37. Wahidi MM, Herth FJF, Ernst A. State of the art: Interventional pulmonology. *Chest*. 2007; 131:261–274. [PubMed: 17218585]
38. Maisels MJ, McDonagh AF. Phototherapy for neonatal jaundice. *N Engl J Med*. 2008; 358:920–928. [PubMed: 18305267]
39. Schwarz T, Beissert S. Milestones in photoimmunology. *J Invest Dermatol*. 2013; 133:E7–E10.
40. Gläser R, et al. UV-B radiation induces the expression of antimicrobial peptides in human keratinocytes in vitro and in vivo. *J Allergy Clin Immunol*. 2009; 123:1117–1123. [PubMed: 19342087]
41. Liu PT, et al. Toll-like receptor triggering of a vitamin D-mediated human antimicrobial response. *Science*. 2006; 311:1770–1773. [PubMed: 16497887]
42. Kripke ML. Antigenicity of murine skin tumors induced by ultraviolet light. *J Natl Cancer Inst*. 1974; 53:1333–1336. [PubMed: 4139281]
43. Stapelberg MPF, Williams RBH, Byrne SN, Halliday GM. The alternative complement pathway seems to be a UVA sensor that leads to systemic immunosuppression. *J Invest Dermatol*. 2009; 129:2694–2701. [PubMed: 19516263]
44. Lim HW, et al. Phototherapy in dermatology: A call for action. *J Am Acad Dermatol*. 2015; 72:1078–1080. [PubMed: 25981004]
45. Johnson-Huang LM, et al. Effective narrow-band UVB radiation therapy suppresses the IL-23/IL-17 axis in normalized psoriasis plaques. *J Invest Dermatol*. 2010; 130:2654–2663. [PubMed: 20555351]
46. Stern RS. Psoralen and ultraviolet a light therapy for psoriasis. *N Engl J Med*. 2007; 357:682–690. [PubMed: 17699818]
47. Norval M, Halliday GM. The consequences of UV-induced immunosuppression for human health. *Photochem Photobiol*. 2011; 87:965–977. [PubMed: 21749399]

48. Becklund BR, Severson KS, Vang SV, DeLuca HF. UV radiation suppresses experimental autoimmune encephalomyelitis independent of vitamin D production. *Proc Natl Acad Sci U S A*. 2010; 107:6418–6423. [PubMed: 20308557]
49. Geldenhuys S, et al. Ultraviolet radiation suppresses obesity and symptoms of metabolic syndrome independently of vitamin D in mice fed a high-fat diet. *Diabetes*. 2014; 63:3759–3769. [PubMed: 25342734]
50. Slusher TM, et al. A Randomized Trial of Phototherapy with Filtered Sunlight in African Neonates. *N Engl J Med*. 2015; 373:1115–1124. [PubMed: 26376136]
51. Anderson JL, Glod Ca, Dai J, Cao Y, Lockley SW. Lux vs. wavelength in light treatment of seasonal affective disorder. *Acta Psychiatr Scand*. 2009; 120:203–212. [PubMed: 19207131]
52. LeGates, Ta, Fernandez, DC., Hattar, S. Light as a central modulator of circadian rhythms, sleep and affect. *Nat Rev Neurosci*. 2014; 15:443–54. [PubMed: 24917305]
53. Golden RN, et al. The efficacy of light therapy in the treatment of mood disorders: a review and meta-analysis of the evidence. *Am J Psychiatry*. 2005; 162:656–662. [PubMed: 15800134]
54. Lockley SW, Brainard GC, Czeisler Ca. High sensitivity of the human circadian melatonin rhythm to resetting by short wavelength light. *J Clin Endocrinol Metab*. 2003; 88:4502–4505. [PubMed: 12970330]
55. Lam RW, et al. Efficacy of Bright Light Treatment, Fluoxetine, and the Combination in Patients With Nonseasonal Major Depressive Disorder. *JAMA Psychiatry*. 2015; 73:1.
56. Dai T, et al. Blue light rescues mice from potentially fatal *Pseudomonas aeruginosa* burn infection: Efficacy, safety, and mechanism of action. *Antimicrob Agents Chemother*. 2013; 57:1238–1245. [PubMed: 23262998]
57. Dai T, et al. Blue light for infectious diseases: *Propionibacterium acnes*, *Helicobacter pylori*, and beyond? *Drug Resist Updat*. 2012; 15:233–236.
58. Wu PC, Tsai CL, Wu HL, Yang YH, Kuo HK. Outdoor activity during class recess reduces myopia onset and progression in school children. *Ophthalmology*. 2013; 120:1080–1085. [PubMed: 23462271]
59. Smith EL, Hung LF, Huang J. Protective effects of high ambient lighting on the development of form-deprivation myopia in rhesus monkeys. *Investig Ophthalmol Vis Sci*. 2012; 53:421–428. [PubMed: 22169102]
60. Wang J, Li B, Wu MX. Effective and lesion-free cutaneous influenza vaccination. *Proc Natl Acad Sci*. 2015; 112:5005–5010. [PubMed: 25848020]
61. Avci P, Gupta GK, Clark J, Wikonkal N, Hamblin MR. Low-level laser (light) therapy (LLLT) for treatment of hair loss. *Lasers Surg Med Surg Med*. 2014; 46:144–151.
62. Chung H, et al. The nuts and bolts of low-level laser (light) therapy. *Ann Biomed Eng*. 2012; 40:516–533. [PubMed: 22045511]
63. Chow RT, Johnson MI, Lopes-Martins RA, Bjordal JM. Efficacy of low-level laser therapy in the management of neck pain: a systematic review and meta-analysis of randomised placebo or active-treatment controlled trials. *Lancet*. 2009; 374:1897–1908. [PubMed: 19913903]
64. Naeser, Ma, et al. Significant improvements in cognitive performance post-transcranial, red/near-infrared light-emitting diode treatments in chronic, mild traumatic brain injury: open-protocol study. *J Neurotrauma*. 2014; 31:1008–1017. [PubMed: 24568233]
65. Arany PR, et al. Photoactivation of endogenous latent transforming growth Factor-beta 1 directs dental stem cell differentiation for regeneration. *Sci Transl Med*. 2014; 6:238ra69.
66. Shapiro MG, Homma K, Villarreal S, Richter CP, Bezanilla F. Infrared light excites cells by changing their electrical capacitance. *Nat Commun*. 2012; 3:736. [PubMed: 22415827]
67. Jenkins MW, et al. Optical pacing of the embryonic heart. *Nat Photonics*. 2010; 4:623–626. [PubMed: 21423854]
68. Teudt IU, Nevel AE, Izzo AD, Walsh JT, Richter CP. Optical stimulation of the facial nerve: a new monitoring technique? *Laryngoscope*. 2007; 117:1641–1647. [PubMed: 17607145]
69. Wollensak G, Spoerl E, Seiler T. Stress-strain measurements of human and porcine corneas after riboflavin – ultraviolet-A-induced cross-linking. *J Cataract Refract Surg*. 2003; 29:1780–1785. [PubMed: 14522301]

70. Lang N, et al. A blood-resistant surgical glue for minimally invasive repair of vessels and heart defects. *Sci Transl Med.* 2014; 6:218ra6.
71. Roche ET, et al. A light-reflecting balloon catheter for atraumatic tissue defect repair. *Sci Transl Med.* 2015; 7:306ra149-306ra149.
72. Du Y, Lo E, Ali S, Khademhosseini A. Directed assembly of cell-laden microgels for fabrication of 3D tissue constructs. *Proc Natl Acad Sci U S A.* 2008; 105:9522–9527. [PubMed: 18599452]
73. Hillel AT, et al. Photoactivated composite biomaterial for soft tissue restoration in rodents and in humans. *Sci Transl Med.* 2011; 3:93ra67.
74. Castano AP, Mroz P, Hamblin MR. Photodynamic therapy and anti-tumour immunity. *Nat Rev Cancer.* 2006; 6:535–545. [PubMed: 16794636]
75. Agostinis P, et al. Photodynamic Therapy of Cancer: An Update. *Ca-a Cancer J Clin.* 2011; 61:250–281.
76. Spring BQ, Rizvi I, Xu N, Hasan T. The role of photodynamic therapy in overcoming cancer drug resistance. *Photochem Photobiol Sci.* 2015; 14:1476–91. [PubMed: 25856800]
77. Wan MT, Lin JY. Current evidence and applications of photodynamic therapy in dermatology. *Clin Cosmet Investig Dermatol.* 2014; 7:145–163.
78. Lozano M, Cid J, Müller TH. Plasma treated with methylene blue and light: Clinical efficacy and safety profile. *Transfus Med Rev.* 2013; 27:235–240. [PubMed: 24075476]
79. Yang Y, et al. Thienopyrrole-expanded BODIPY as a potential NIR photosensitizer for photodynamic therapy. *Chem Commun (Camb).* 2013; 49:3940–2. [PubMed: 23536148]
80. Idris NM, et al. In vivo photodynamic therapy using upconversion nanoparticles as remote-controlled nanotransducers. *Nat Med.* 2012; 18:1580–1585. [PubMed: 22983397]
81. Kim YR, et al. Bioluminescence-activated deep-tissue photodynamic therapy of cancer. *Theranostics.* 2015; 5:805–817. [PubMed: 26000054]
82. Hildebrandt B. The cellular and molecular basis of hyperthermia. *Crit Rev Oncol Hematol.* 2002; 43:33–56. [PubMed: 12098606]
83. Jin CS, Lovell JF, Chen J, Zheng G. Ablation of Hypoxic Tumors with Dose-Equivalent Photothermal, but Not Photodynamic, Therapy Using a Nanostructured Porphyrin Assembly. *ACS Nano.* 2013; 7:2541–2550. [PubMed: 23394589]
84. Huang X, El-Sayed IH, Qian W, El-Sayed Ma. Cancer cell imaging and photothermal therapy in the near-infrared region by using gold nanorods. *J Am Chem Soc.* 2006; 128:2115–2120. [PubMed: 16464114]
85. Cheng L, Yang K, Chen Q, Liu Z. Organic stealth nanoparticles for highly effective in vivo near-infrared photothermal therapy of cancer. *ACS Nano.* 2012; 6:5605–5613. [PubMed: 22616847]
86. Lovell JF, et al. Porphysome nanovesicles generated by porphyrin bilayers for use as multimodal biophotonic contrast agents. *Nat Mater.* 2011; 10:324–332. [PubMed: 21423187]
87. Shaikh N, Hoberman A, Kaleida PH, Ploof DL, Paradise JL. Diagnosing otitis media — otoscopy and cerumen removal. *N Engl J Med.* 2010; 362:e62. [PubMed: 20484393]
88. Thangaratnam S, Brown K, Zamora J, Khan KS, Ewer AK. Pulse oximetry screening for critical congenital heart defects in asymptomatic newborn babies: A systematic review and meta-analysis. *Lancet.* 2012; 379:2459–2464. [PubMed: 22554860]
89. Boas, Da, Elwell, CE., Ferrari, M., Taga, G. Twenty years of functional near-infrared spectroscopy: Introduction for the special issue. *Neuroimage.* 2014; 85:1–5. [PubMed: 24321364]
90. Schwarz, Ra, et al. Noninvasive evaluation of oral lesions using depth-sensitive optical spectroscopy. *Cancer.* 2009; 115:1669–1679. [PubMed: 19170229]
91. Humeau-Heurtier A, Guerreschi E, Abraham P, Mahé G. Relevance of laser doppler and laser speckle techniques for assessing vascular function: State of the art and future trends. *IEEE Trans Biomed Eng.* 2013; 60:659–666. [PubMed: 23372072]
92. Bolay H, et al. Intrinsic brain activity triggers trigeminal meningeal afferents in a migraine model. *Nat Med.* 2002; 8:136–142. [PubMed: 11821897]
93. Boppart SA, Richards-Kortum R. Point-of-care and point-of-procedure optical imaging technologies for primary care and global health. *Sci Transl Med.* 2014; 6:253rv2.

94. Greenbaum A, et al. Wide-field computational imaging of pathology slides using lens-free on-chip microscopy. *Sci Transl Med*. 2014; 6:267ra175.
95. Shen L, Hagen Ja, Papautsky I. Point-of-care colorimetric detection with a smartphone. *Lab Chip*. 2012; 12:4240. [PubMed: 22996728]
96. Ming K, Ming K. An Integrated Quantum Dot Barcode Smartphone Optical Device for Wireless Multiplexed Diagnosis of Infected Patients by for Wireless Multiplexed Diagnosis of Infected Patients. 2015:3060–3074.
97. Ambrosio MVD, et al. Point-of-care quantification of blood-borne filarial parasites with a mobile phone microscope. *Sci Transl Med*. 2015; 7:286re4.
98. Bao J, Bawendi MG. A colloidal quantum dot spectrometer. *Nature*. 2013; 523:67–70.
99. Shelton RL, et al. Optical coherence tomography for advanced screening in the primary care office. *J Biophotonics*. 2014; 7:525–533. [PubMed: 23606343]
100. de la Rica R, Stevens MM. Plasmonic ELISA for the ultrasensitive detection of disease biomarkers with the naked eye. *Nat Nanotechnol*. 2012; 8:1759–1764.
101. Chen Z, et al. Protein microarrays with carbon nanotubes as multicolor Raman labels. *Nat Biotechnol*. 2008; 26:1285–92. [PubMed: 18953353]
102. Armani AM, Kulkarni RP, Fraser SE, Flagan RC, Vahala KJ. Detection with optical microcavities. *Science*. 2007; 317:783–787. [PubMed: 17615303]
103. Fan X, Yun SH. The potential of optofluidic biolasers. *Nat Methods*. 2014; 11:141–7. [PubMed: 24481219]
104. Crosetto N, Bienko M, van Oudenaarden A. Spatially resolved transcriptomics and beyond. *Nat Rev Genet*. 2015; 16:57–66. [PubMed: 25446315]
105. Friedman, Aa, Letai, A., Fisher, DE., Flaherty, KT. Precision medicine for cancer with next-generation functional diagnostics. *Nat Rev Cancer*. 2015; 15:747–756. [PubMed: 26536825]
106. Veitch AM, Uedo N, Yao K, East JE. Optimizing early upper gastrointestinal cancer detection at endoscopy. *Nat Rev Gastroenterol Hepatol*. 2015; 12:660–7. [PubMed: 26260369]
107. Deepak P, et al. Incremental diagnostic yield of chromoendoscopy and outcomes in inflammatory bowel disease patients with a history of colorectal dysplasia on white-light endoscopy. *Gastrointest Endosc*. 2016; 83:1005–1012. [PubMed: 26408903]
108. Iddan G, Meron G, Glukhovskiy A, Swain P. Wireless capsule endoscopy. *Nature*. 2000; 405:417.
109. Liao Z, Gao R, Xu C, Li ZS. Indications and detection, completion, and retention rates of small-bowel capsule endoscopy: a systematic review. *Gastrointest Endosc*. 2010; 71:280–286. [PubMed: 20152309]
110. Drexler W, Fujimoto JG. State-of-the-art retinal optical coherence tomography. *Prog Retin Eye Res*. 2008; 27:45–88. [PubMed: 18036865]
111. Huang D, et al. Optical coherence tomography. *Science*. 1991; 254:1178–1181. [PubMed: 1957169]
112. Yun SH, et al. Comprehensive volumetric optical microscopy in vivo. *Nat Med*. 2006; 12:1429–1433. [PubMed: 17115049]
113. Tearney GJ, et al. Consensus standards for acquisition, measurement, and reporting of intravascular optical coherence tomography studies: a report from the International Working Group for Intravascular Optical Coherence Tomography Standardization and Validation. *J Am Coll Cardiol*. 2012; 59:1058–1072. [PubMed: 22421299]
114. Prati F, et al. Expert review document part 2: Methodology, terminology and clinical applications of optical coherence tomography for the assessment of interventional procedures. *Eur Heart J*. 2012; 33:2513–2520. [PubMed: 22653335]
115. Bouma BE, Tearney GJ, Compton CC, Nishioka NS. High-resolution imaging of the human esophagus and stomach in vivo using optical coherence tomography. *Gastrointest Endosc*. 2000; 51:467–474. [PubMed: 10744824]
116. Liu L, et al. Imaging the subcellular structure of human coronary atherosclerosis using micro-optical coherence tomography. *Nat Med*. 2011; 17:1010–1014. [PubMed: 21743452]
117. Yoo H, et al. Intra-arterial catheter for simultaneous microstructural and molecular imaging in vivo. *Nat Med*. 2011; 17:1680–4. [PubMed: 22057345]



118. Roblyer D, et al. Optical imaging of breast cancer oxyhemoglobin flare correlates with neoadjuvant chemotherapy response one day after starting treatment. *Proc Natl Acad Sci.* 2011; 108:14626–14631. [PubMed: 21852577]
119. Schaafsma BE, et al. Optical mammography using diffuse optical spectroscopy for monitoring tumor response to neoadjuvant chemotherapy in women with locally advanced breast cancer. *Clin Cancer Res.* 2015; 21:577–584. [PubMed: 25473002]
120. Jiang S, et al. Predicting breast tumor response to neoadjuvant chemotherapy with diffuse optical spectroscopic tomography prior to treatment. *Clin Cancer Res.* 2014; 20:6006–6015. [PubMed: 25294916]
121. Fang Q, et al. Combined optical and X-ray tomosynthesis breast imaging. *Radiology.* 2011; 258:89–97. [PubMed: 21062924]
122. Eggebrecht AT, et al. Mapping distributed brain function and networks with diffuse optical tomography. *Nat Photonics.* 2014; 8:448–454. [PubMed: 25083161]
123. White BR, Liao SM, Ferradal SL, Inder TE, Culver JP. Bedside optical imaging of occipital resting-state functional connectivity in neonates. *Neuroimage.* 2012; 59:2529–2538. [PubMed: 21925609]
124. Kiesslich R, et al. Confocal laser endoscopy for diagnosing intraepithelial neoplasias and colorectal cancer in vivo. *Gastroenterology.* 2004; 127:706–713. [PubMed: 15362025]
125. Buchner AM, et al. Comparison of probe-based confocal laser endomicroscopy with virtual chromoendoscopy for classification of colon polyps. *Gastroenterology.* 2010; 138:834–842. [PubMed: 19909747]
126. Moussata D, et al. Confocal laser endomicroscopy is a new imaging modality for recognition of intramucosal bacteria in inflammatory bowel disease in vivo. *Gut.* 2011; 60:26–33. [PubMed: 20980342]
127. Sonn, Ga, et al. Optical biopsy of human bladder neoplasia with in vivo confocal laser endomicroscopy. *J Urol.* 2009; 182:1299–1305. [PubMed: 19683270]
128. Hsiung PL, et al. Detection of colonic dysplasia in vivo using a targeted heptapeptide and confocal microendoscopy. *Nat Med.* 2008; 14:454–458. [PubMed: 18345013]
129. Sturm MB, et al. Targeted imaging of esophageal neoplasia with a fluorescently labeled peptide: first-in-human results. *Sci Transl Med.* 2013; 5:184ra61.
130. Bird-Lieberman EL, et al. Molecular imaging using fluorescent lectins permits rapid endoscopic identification of dysplasia in Barrett’s esophagus. *Nat Med.* 2012; 18:315–21. [PubMed: 22245781]
131. Pan Y, et al. Endoscopic molecular imaging of human bladder cancer using a CD47 antibody. *Sci Transl Med.* 2014; 6:260ra148.
132. Burggraaf J, et al. Detection of colorectal polyps in humans using an intravenously administered fluorescent peptide targeted against c-Met. *Nat Med.* 2015; 21:955–961. [PubMed: 26168295]
133. Fitzgerald R. Assessing the potential impact of fluorescence angiography in preventing limb loss. *Pod Today.* 2016; 29
134. Choi M, Kwok SJJ, Yun SH. In vivo fluorescence microscopy: lessons from observing cell behavior in their native environment. *Physiology.* 2015; 30:40–49. [PubMed: 25559154]
135. Dimitrow E, et al. Sensitivity and specificity of multiphoton laser tomography for in vivo and ex vivo diagnosis of malignant melanoma. *J Invest Dermatol.* 2009; 129:1752–1758. [PubMed: 19177136]
136. Palczewska G, et al. Noninvasive two-photon microscopy imaging of mouse retina and retinal pigment epithelium through the pupil of the eye. *Nat Med.* 2014; 20:785–789. [PubMed: 24952647]
137. Saar BG, et al. Video-rate molecular imaging in vivo with stimulated Raman scattering. *Science.* 2010; 330:1368–1370. [PubMed: 21127249]
138. Ji M, et al. Detection of human brain tumor infiltration with quantitative stimulated Raman scattering microscopy. *Sci Transl Med.* 2015; 7:309ra163.
139. Yao J, et al. High-speed label-free functional photoacoustic microscopy of mouse brain in action. *Nat Methods.* 2015; 12:407–410. [PubMed: 25822799]

140. Yang JM, et al. Simultaneous functional photoacoustic and ultrasonic endoscopy of internal organs in vivo. *Nat Med.* 2012; 18:1297–1302. [PubMed: 22797808]
141. Galanzha EI, et al. In vivo magnetic enrichment and multiplex photoacoustic detection of circulating tumour cells. *Nat Nanotechnol.* 2009; 4:855–860. [PubMed: 19915570]
142. Ermilov, Sa, et al. Laser optoacoustic imaging system for detection of breast cancer. *J Biomed Opt.* 2009; 14:24007.
143. Kitai T, et al. Photoacoustic mammography: Initial clinical results. *Breast Cancer.* 2014; 21:146–153. [PubMed: 22484692]
144. Scope A, et al. In vivo reflectance confocal microscopy of shave biopsy wounds: feasibility of intraoperative mapping of cancer margins. *Br J Dermatol.* 2010; 163:1218–1228. [PubMed: 20874785]
145. Guitera P, et al. In vivo confocal microscopy for diagnosis of melanoma and basal cell carcinoma using a two-step method: analysis of 710 consecutive clinically equivocal cases. *J Invest Dermatol.* 2012; 132:2386–2394. [PubMed: 22718115]
146. Scarcelli G, Besner S, Pineda R, Kalout P, Yun SH. In vivo biomechanical mapping of normal and keratoconus corneas. *JAMA Ophthalmol.* 2015; 133:480–482. [PubMed: 25611213]
147. Tsui C, Klein R, Garabrant M. Minimally invasive surgery: national trends in adoption and future directions for hospital strategy. *Surg Endosc Other Interv Tech.* 2013; 27:2253–2257.
148. Omata J, et al. Acute gastric volvulus associated with wandering spleen in an adult treated laparoscopically after endoscopic reduction: a case report. *Surg Case Reports.* 2016; 2:47.
149. Jourdan IC, et al. Stereoscopic vision provides a significant advantage for precision robotic laparoscopy. *Br J Surg.* 2004; 91:879–885. [PubMed: 15227695]
150. Vahrmeijer AL, Hutteman M, van der Vorst JR, van de Velde CJH, Frangioni JV. Image-guided cancer surgery using near-infrared fluorescence. *Nat Rev Clin Oncol.* 2013; 10:507–18. [PubMed: 23881033]
151. Nguyen QT, Tsien RY. Fluorescence-guided surgery with live molecular navigation—a new cutting edge. *Nat Rev Cancer.* 2013; 13:653–62. [PubMed: 23924645]
152. Widhalm G, et al. 5-Aminolevulinic acid induced fluorescence Is a powerful intraoperative marker for precise histopathological grading of gliomas with non-significant contrast-enhancement. *PLoS One.* 2013; 8
153. Stummer W, et al. Fluorescence-guided surgery with 5-aminolevulinic acid for resection of malignant glioma: a randomised controlled multicentre phase III trial. *Lancet Oncol.* 2006; 7:392–401. [PubMed: 16648043]
154. Choi HS, et al. Targeted zwitterionic near-infrared fluorophores for improved optical imaging. *Nat Biotechnol.* 2013; 31:148–153. [PubMed: 23292608]
155. Hyun H, et al. Structure-inherent targeting of near-infrared fluorophores for parathyroid and thyroid gland imaging. *Nat Med.* 2015; 21:192–197. [PubMed: 25559343]
156. Verbeek FPR, et al. Near-infrared fluorescence sentinel lymph node mapping in breast cancer: a multicenter experience. *Breast Cancer Res Treat.* 2014; 143:333–42. [PubMed: 24337507]
157. Van Der Vorst JR, et al. Near-infrared fluorescence-guided resection of colorectal liver metastases. *Cancer.* 2013; 119:3411–3418. [PubMed: 23794086]
158. van Dam GM, et al. Intraoperative tumor-specific fluorescence imaging in ovarian cancer by folate receptor- $\alpha$  targeting: first in-human results. *Nat Med.* 2011; 17:1315–1319. [PubMed: 21926976]
159. Metildi, Ca, et al. Ratiometric activatable cell-penetrating peptides label pancreatic cancer, enabling fluorescence-guided surgery, which reduces metastases and recurrence in orthotopic mouse models. *Ann Surg Oncol.* 2014; 22:2082–2087. [PubMed: 25319581]
160. Whitney, Ma, et al. Fluorescent peptides highlight peripheral nerves during surgery in mice. *Nat Biotechnol.* 2011; 29:352–356. [PubMed: 21297616]
161. Weissleder R, Tung CH, Mahmood U, Bogdanov A. In vivo imaging of tumors with protease-activated near-infrared fluorescent probes. *Nat Biotechnol.* 1999; 17:375–378. [PubMed: 10207887]

162. Whitley MJ, et al. A mouse-human phase 1 co-clinical trial of a protease-activated fluorescent probe for imaging cancer. *Sci Transl Med.* 2016; 8:320ra4.
163. Ehlers JP, et al. The prospective intraoperative and perioperative ophthalmic imaging with optical coherence tomography (PIONEER) study: 2-year results. *Am J Ophthalmol.* 2014; 158:999–1007. [PubMed: 25077834]
164. Prati F, et al. Angiography alone versus angiography plus optical coherence tomography to guide decision-making during percutaneous coronary intervention: The Centro per la Lotta contro l'Infarto-Optimisation of Percutaneous Coronary Intervention (CLI-OPCI) study. *EuroIntervention.* 2012; 8:823–829. [PubMed: 23034247]
165. Kut C, et al. Detection of human brain cancer infiltration ex vivo and in vivo using quantitative optical coherence tomography. *Sci Transl Med.* 2015; 7:292ra100.
166. Ji M, et al. Rapid, label-free detection of brain tumors with stimulated Raman scattering microscopy. *Sci Transl Med.* 2013; 5:201ra119.
167. Jermyn M, et al. Intraoperative brain cancer detection with Raman spectroscopy in humans. *Sci Transl Med.* 2015; 7:274ra19.
168. Celli JP, et al. Imaging and photodynamic therapy: mechanisms, monitoring, and optimization. *Chem Rev.* 2010; 110:2795–2838. [PubMed: 20353192]
169. Yang VXD, Muller PJ, Herman P, Wilson BC. A multispectral fluorescence imaging system: Design and initial clinical tests in intra-operative photofrin-photodynamic therapy of brain tumors. *Lasers Surg Med.* 2003; 32:224–232. [PubMed: 12605430]
170. Ntziachristos V, et al. Visualization of antitumor treatment by means of fluorescence molecular tomography with an annexin V-Cy5.5 conjugate. *Proc Natl Acad Sci U S A.* 2004; 101:12294–12299. [PubMed: 15304657]
171. Atreya R, et al. In vivo imaging using fluorescent antibodies to tumor necrosis factor predicts therapeutic response in Crohn's disease. *Nat Med.* 2014; 20:313–318. [PubMed: 24562382]
172. Zhang R, et al. Real-time in vivo Cherenkovscopy imaging during external beam radiation therapy. *J Biomed Opt.* 2013; 18:110504. [PubMed: 24247743]
173. Grotjohann T, et al. Diffraction-unlimited all-optical imaging and writing with a photochromic GFP. *Nature.* 2011; 478:204–8. [PubMed: 21909116]
174. Chen BC, et al. Lattice light-sheet microscopy: imaging molecules to embryos at high spatiotemporal resolution. *Science.* 2014; 346:439.
175. Yang B, et al. Single-cell phenotyping within transparent intact tissue through whole-body clearing. *Cell.* 2014; 158:945–958. [PubMed: 25088144]
176. Mosk AP, Lagendijk A, Lerosey G, Fink M. Controlling waves in space and time for imaging and focusing in complex media. *Nat Photonics.* 2012; 6:283–292.
177. Doane TL, Burda C. The unique role of nanoparticles in nanomedicine: imaging, drug delivery and therapy. *Chem Soc Rev.* 2012; 41:2885. [PubMed: 22286540]
178. Youan BBC. Chronopharmaceutical drug delivery systems: Hurdles, hype or hope? *Adv Drug Deliv Rev.* 2010; 62:898–903. [PubMed: 20438781]
179. Jayakumar MKG, Idris NM, Zhang Y. Remote activation of biomolecules in deep tissues using near-infrared-to-UV upconversion nanotransducers. *Proc Natl Acad Sci.* 2012; 109:8483–8488. [PubMed: 22582171]
180. Yavuz MS, et al. Gold nanocages covered by smart polymers for controlled release with near-infrared light. *Nat Mater.* 2009; 8:935–939. [PubMed: 19881498]
181. Carter KA, et al. Porphyrin-phospholipid liposomes permeabilized by near-infrared light. *Nat Commun.* 2014; 5:3546. [PubMed: 24699423]
182. Li Y, et al. A smart and versatile theranostic nanomedicine platform based on nanoporphyrin. *Nat Commun.* 2014; 5:4712. [PubMed: 25158161]
183. Phillips E, et al. Clinical translation of an ultras-small inorganic optical-PET imaging nanoparticle probe. *Sci Transl Med.* 2014; 6:260ra149.
184. Kircher MF, et al. A brain tumor molecular imaging strategy using a new triple-modality MRI-photoacoustic-Raman nanoparticle. *Nat Med.* 2012; 18:829–834. [PubMed: 22504484]

185. Lin J, et al. Photosensitizer-loaded gold vesicles with strong plasmonic coupling effect for imaging-guided photothermal/photodynamic therapy. *ACS Nano*. 2013; 7:5320–5329. [PubMed: 23721576]
186. Liu J, et al. Bismuth Sulfide Nanorods as a Precision Nanomedicine for in Vivo Multimodal Imaging-Guided Photothermal Therapy of Tumor. *ACS Nano*. 2015; 9:696–707. [PubMed: 25561009]
187. Spring BQ, et al. A photoactivable multi-inhibitor nanoliposome for tumour control and simultaneous inhibition of treatment escape pathways. *Nat Nanotechnol*. 2016; 11:378–387. [PubMed: 26780659]
188. Pasparakis G, Manouras T, Vamvakaki M, Argitis P. Harnessing photochemical internalization with dual degradable nanoparticles for combinatorial photo-chemotherapy. *Nat Commun*. 2014; 5:3623. [PubMed: 24710504]
189. Lukianova-Hleb EY, et al. On-demand intracellular amplification of chemoradiation with cancer-specific plasmonic nanobubbles. *Nat Med*. 2014; 20:778–784. [PubMed: 24880615]
190. Wilhelm S, et al. Analysis of nanoparticle delivery to tumours. *Nat Rev Mater*. 2016; 1:16014.
191. Tong R, Langer R. Nanomedicines targeting the tumor microenvironment. *Cancer J*. 2015; 21:314–321. [PubMed: 26222084]
192. Douglas SM, Bachelet I, Church GM. Transport of molecular payloads. *Science*. 2012; 335:831–834. [PubMed: 22344439]
193. von Maltzahn G, et al. Nanoparticles that communicate in vivo to amplify tumour targeting. *Nat Mater*. 2011; 10:545–552. [PubMed: 21685903]
194. Dai B, et al. Programmable artificial phototactic microswimmer. *Nat Nanotechnol*. 2016; doi: 10.1038/nnano.2016.187
195. Boyden ES, Zhang F, Bamberg E, Nagel G, Deisseroth K. Millisecond-timescale, genetically targeted optical control of neural activity. *Nat Neurosci*. 2005; 8:1263–1268. [PubMed: 16116447]
196. Gradinaru V, Mogri M, Thompson KR, Henderson JM, Deisseroth K. Optical deconstruction of parkinsonian neural circuitry. *Science*. 2009; 324:354–359. [PubMed: 19299587]
197. Creed M, Pascoli VJ, Luscher C. Refining deep brain stimulation to emulate optogenetic treatment of synaptic pathology. *Science*. 2015; 347:659–664. [PubMed: 25657248]
198. Williams JC, Denison T. From optogenetic technologies to neuromodulation therapies. *Sci Transl Med*. 2013; 5:177ps6.
199. Chow BY, Boyden ES. Optogenetics and Translational Medicine. *Sci Transl Med*. 2013; 5:177ps5.
200. Ramirez S, et al. Activating positive memory engrams suppresses depression-like behaviour. *Nature*. 2015; 522:335–339. [PubMed: 26085274]
201. Iyer SM, et al. Virally mediated optogenetic excitation and inhibition of pain in freely moving nontransgenic mice. *Nat Biotechnol*. 2014; 32:274–278. [PubMed: 24531797]
202. Bruegmann T, et al. Optogenetic control of contractile function in skeletal muscle. *Nat Commun*. 2015; 6:7153. [PubMed: 26035411]
203. Busskamp V, Roska B. Optogenetic approaches to restoring visual function in retinitis pigmentosa. *Curr Opin Neurobiol*. 2011; 21:942–946. [PubMed: 21708457]
204. Barrett JM, Berlinguer-Palmini R, Degenaar P. Optogenetic approaches to retinal prosthesis. *Vis Neurosci*. 2014; 31:345–54. [PubMed: 25100257]
205. Kramer RH, Mourot A, Adesnik H. Optogenetic pharmacology for control of native neuronal signaling proteins. *Nat Neurosci*. 2013; 16:816–23. [PubMed: 23799474]
206. Polosukhina A, et al. Photochemical Restoration of Visual Responses in Blind Mice. *Neuron*. 2012; 75:271–282. [PubMed: 22841312]
207. Mourot A, et al. Rapid optical control of nociception with an ion-channel photoswitch. *Nat Methods*. 2012; 9:396–402. [PubMed: 22343342]
208. Levitz J, et al. Optical control of metabotropic glutamate receptors. *Nat Neurosci*. 2013; 16:507–16. [PubMed: 23455609]

209. Gaub BM, et al. Restoration of visual function by expression of a light-gated mammalian ion channel in retinal ganglion cells or ON-bipolar cells. *Proc Natl Acad Sci.* 2014; 111:E5574–E5583. [PubMed: 25489083]
210. Melyan Z, Tarttelin EE, Bellingham J, Lucas RJ, Hankins MW. Addition of human melanopsin renders mammalian cells photoresponsive. *Nature.* 2005; 433:741–745. [PubMed: 15674244]
211. Ye H, Daoud-El Baba M, Peng RW, Fussenegger M. A synthetic optogenetic transcription device enhances blood-glucose homeostasis in mice. *Science.* 2011; 332:1565–1568. [PubMed: 21700876]
212. Choi M, et al. Light-guiding hydrogels for cell-based sensing and optogenetic synthesis in vivo. *Nat Photonics.* 2013; 7:987–994. [PubMed: 25346777]
213. Gao L, et al. Epidermal photonic devices for quantitative imaging of temperature and thermal transport characteristics of the skin. *Nat Commun.* 2014; 5:4938. [PubMed: 25234839]
214. White MS, et al. Ultrathin, highly flexible and stretchable PLEDs. *Nat Photonics.* 2013; 7:811–816.
215. Wang C, et al. User-interactive electronic skin for instantaneous pressure visualization. *Nat Mater.* 2013; 12:899–904. [PubMed: 23872732]
216. Lochner CM, Khan Y, Pierre A, Arias AC. (UC B All-organic optoelectronic sensor for pulse oximetry. *Nat Commun.* 2014; 5:5745. [PubMed: 25494220]
217. Kim J, et al. Battery-free, stretchable optoelectronic systems for wireless optical characterization of the skin. *Sci Adv.* 2016; 2:e1600418. [PubMed: 27493994]
218. Lee H, et al. An endoscope with integrated transparent bioelectronics and theranostic nanoparticles for colon cancer treatment. *Nat Commun.* 2015; 6:10059. [PubMed: 26616435]
219. Mathieson K, et al. Photovoltaic retinal prosthesis with high pixel density. *Nat Photonics.* 2012; 6:391–397. [PubMed: 23049619]
220. Kim RH, et al. Waterproof AlInGaP optoelectronics on stretchable substrates with applications in biomedicine and robotics. *Nat Mater.* 2010; 9:929–937. [PubMed: 20953185]
221. Kim T, et al. Injectable, cellular-scale optoelectronics with applications for wireless optogenetics. *Science.* 2013; 340:211–216. [PubMed: 23580530]
222. Montgomery KL, et al. Wirelessly powered, fully internal optogenetics for brain, spinal and peripheral circuits in mice. *Nat Methods.* 2015; 12:969–974. [PubMed: 26280330]
223. Park SI, et al. Soft, stretchable, fully implantable miniaturized optoelectronic systems for wireless optogenetics. *Nat Biotechnol.* 2015; 33:1280–1286. [PubMed: 26551059]
224. Jeong JW, et al. Wireless optofluidic systems for programmable in vivo pharmacology and optogenetics. *Cell.* 2015; 162:662–674. [PubMed: 26189679]
225. Folcher M, et al. Mind-controlled transgene expression by a wireless-powered optogenetic designer cell implant. *Nat Commun.* 2014; 5:1–11.
226. Ho JS, et al. Wireless power transfer to deep-tissue microimplants. *Proc Natl Acad Sci.* 2014; 111:7974–7979. [PubMed: 24843161]
227. Lee SH, Jeong CK, Hwang GT, Lee KJ. Self-powered flexible inorganic electronic system. *Nano Energy.* 2014; 14:111–125.
228. Bae B, et al. Polymeric photosensitizer-embedded self-expanding metal stent for repeatable endoscopic photodynamic therapy of cholangiocarcinoma. *Biomaterials.* 2014; 35:8487–8495. [PubMed: 25043500]
229. Choi M, Humar M, Kim S, Yun SH. Step-index optical fiber made of biocompatible hydrogels. *Adv Mater.* 2015; 27:4081–4086. [PubMed: 26045317]
230. Nizamoglu S, et al. Bioabsorbable polymer optical waveguides for deep-tissue photomedicine. *Nat Commun.* 2015; 7:10374.
231. Canales A, et al. Multifunctional fibers for simultaneous optical, electrical and chemical interrogation of neural circuits in vivo. *Nat Biotechnol.* 2015; 33:277–284. [PubMed: 25599177]
232. Humar M, Yun SH. Intracellular microlasers. *Nat Photonics.* 2015; 9:572–576. [PubMed: 26417383]
233. Cho S, Humar M, Martino N, Yun SH. Laser particle stimulated emission microscopy. *Phys Rev Lett.* 2016; 117

234. van Allen HW. Some new applications of electricity and light in medicine. *N Engl J Med.* 1909; 160:331–333.
235. Jacques SL. Optical properties of biological tissues: a review. *Phys Med Biol.* 2013; 58:R37–61. [PubMed: 23666068]
236. Moritz AR, Henriques FCJ. Studies of thermal Injury II. The relative importance of time and surface temperature in the causation of cutaneous burns. *Am J Pathol.* 1947; 23:695–720. [PubMed: 19970955]
237. Srinivasan R. Ablation of polymers and biological tissue by ultraviolet lasers. *Science.* 1986; 234:559–565. [PubMed: 3764428]
238. Cain CP, et al. ICNIRP guidelines: revision of guidelines on limits of exposure to laser radiation of wavelengths between 400 nm and 1.4  $\mu$ m. *Health Phys.* 2000; 79:431–440. [PubMed: 11007467]
239. Thekaekara MP. Solar radiation measurement: techniques and instrumentation. *Sol Energy.* 1976; 18:309–325.



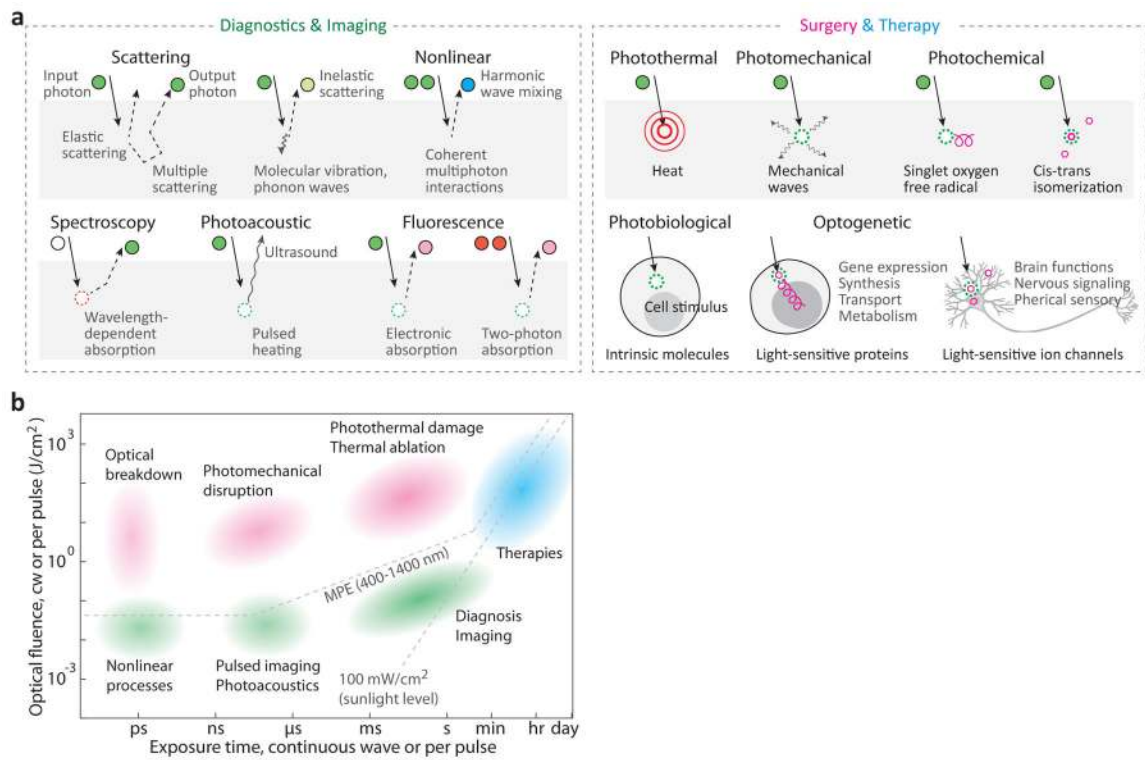


**Figure 1.** Light–tissue interactions. **a**, Representative optical mechanisms used in diagnosis and imaging (left), and surgery and therapy (right). Circular objects denote incoming and outgoing photons, with their trajectories indicated by solid and dotted lines with arrowheads. Circle colours represent the spectrum of the light; dotted circles indicate the absorption of input photons. For the case of therapy, specific effects of light on tissue and cells are indicated. **b**, Optical techniques mapped according to their optical fluence and exposure time (either total illumination time for cw light, or pulse duration for pulses). Background colours represent medical areas: green for diagnostics, magenta for surgery, and cyanine for therapy. MPE, maximum permissible exposure.

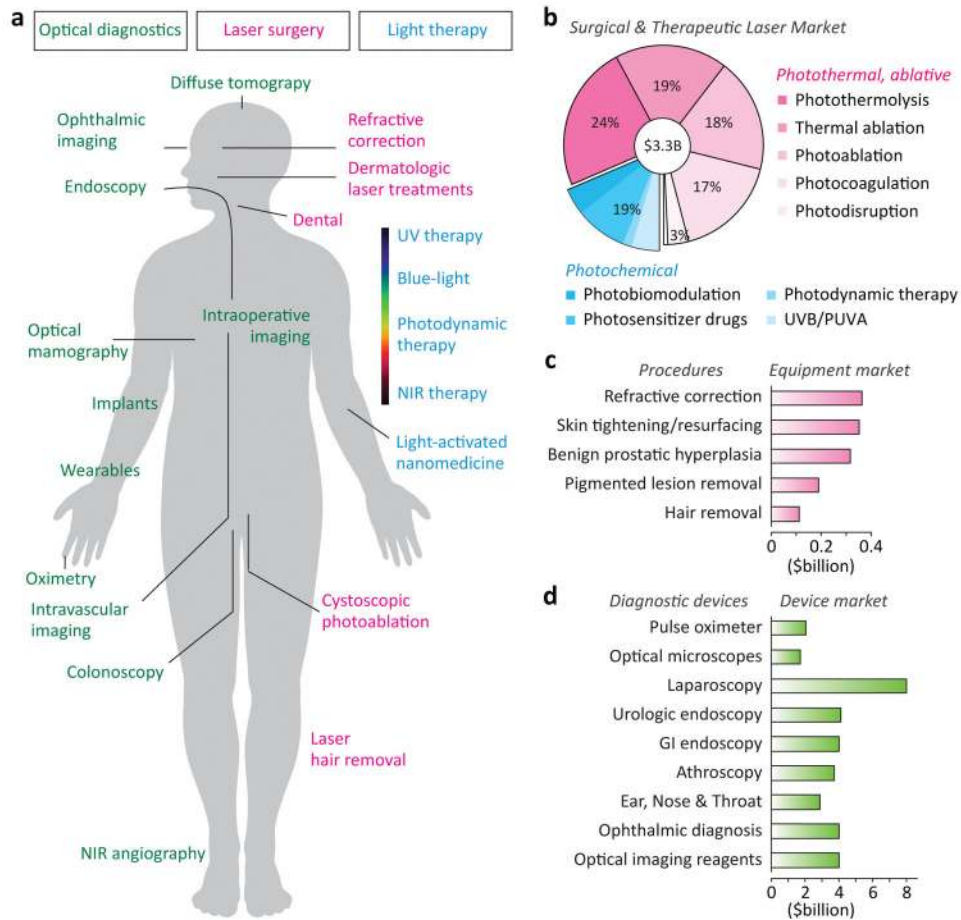


**Figure 2.** Medical application areas of light. **a**, Representative applications of light in the human body for diagnosis and imaging (green), surgery (magenta) and therapy (cyanine). **b**, Global market in 2014 for medical lasers by therapeutic application. Photosensitizer drugs are included as part of the PDT market. **c**, Equipment spending in 2013 for leading laser-treatment procedures. **d**, Global market in 2013–2014 for several major diagnostic devices. Data sources: BCC Research reports HLC093C, HLC072C, and HLC172A (with permission of BCC Research, Wesley, MA, USA).

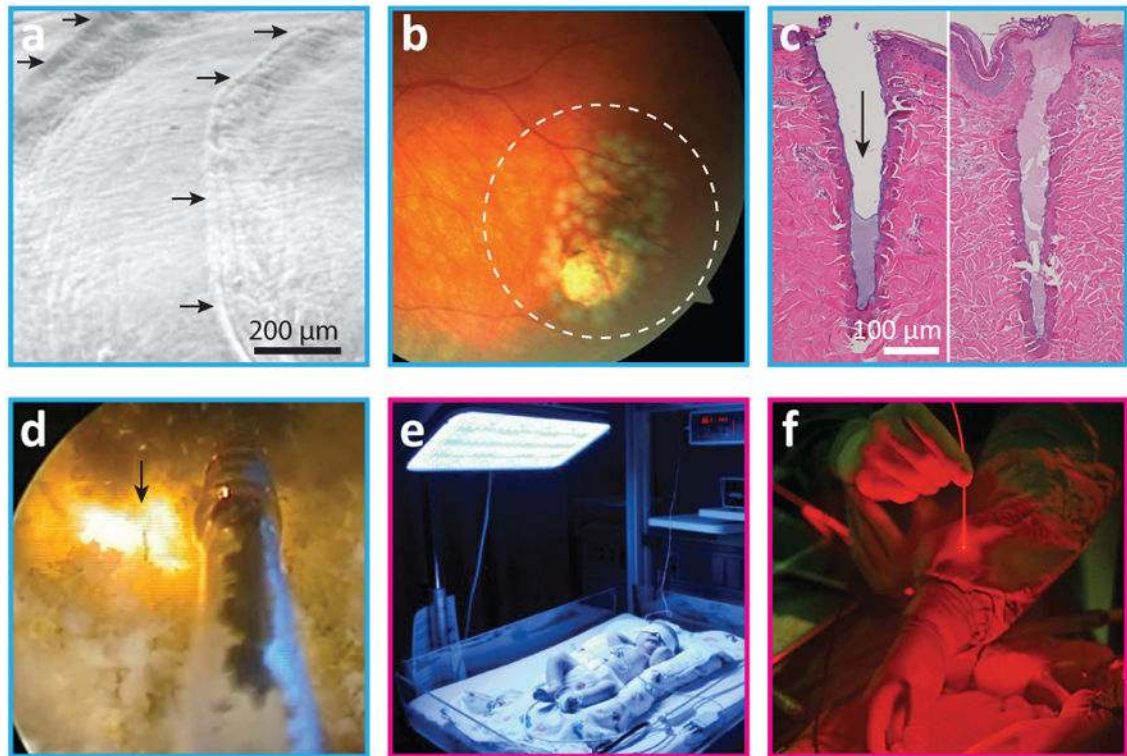


**Figure 3.**

Surgical and therapeutic applications of light. **a**, Photoablation. The scanning electron micrograph shows stepwise ablated patterns (arrows) in an experimental cornea by excimer laser irradiation<sup>4</sup>. **b**, Photocoagulation. Laser-induced damage spots around a retinal tear region<sup>7</sup> (dashed-line circle). **c**, Photothermal ablation. Histology of porcine skin tissues harvested 0 min (left) and 60 min (right) after fractional, pulsed CO<sub>2</sub> laser exposure *in vivo*<sup>16</sup>. The arrow indicates the laser channel, which is filled with fibrin plug within minutes. **d**, Photothermal ablation (vaporization). A fibre-optic catheter delivers high-power continuous-wave laser (arrow) to remove excess prostate tissue in a patient with benign prostate hyperplasia [from Feldman, RG. Prostata laser verde green light. [www.youtube.com/watch?v=jAbSwtSN9xE](http://www.youtube.com/watch?v=jAbSwtSN9xE). License at <http://creativecommons.org/licenses/by/3.0/>]. **e**, Blue-light therapy for the treatment of neonatal jaundice. **f**, Photodynamic therapy. Close-up image of a surgeon's hands in an operating room. Panel **e** reproduced with permission from Photobiological Sciences Online. Panel **f** courtesy of the National Cancer Institute.



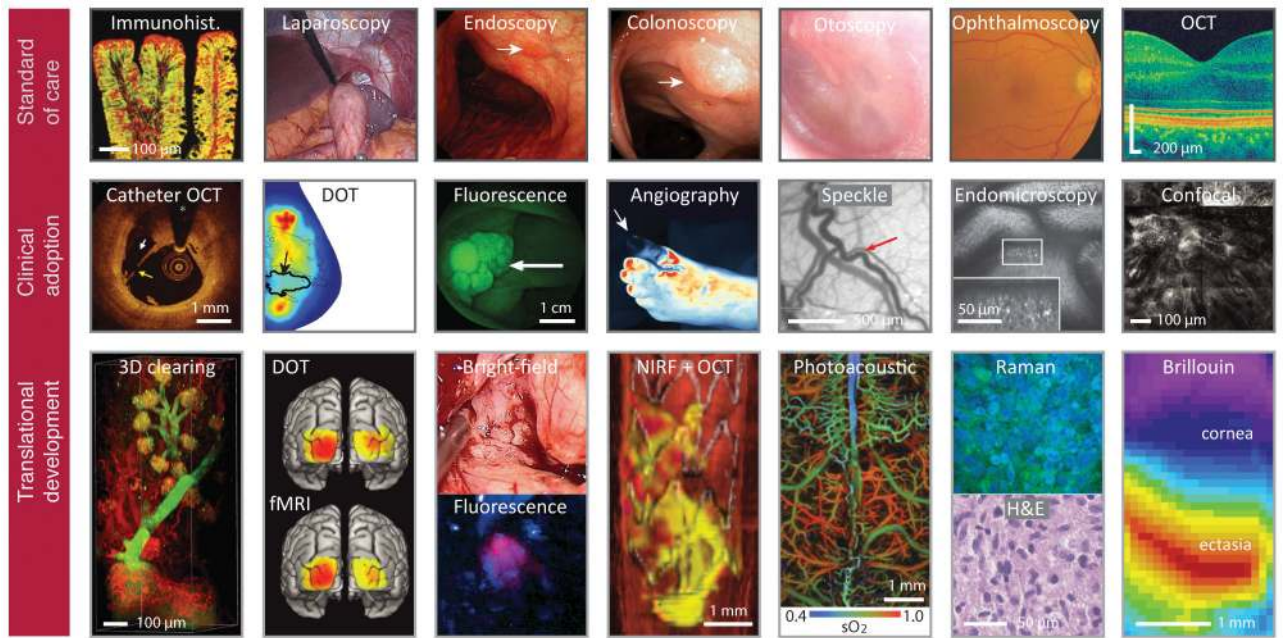


**Figure 4.**

Current and emerging optical imaging. Top row, Established microscopy and endoscopy in routine clinical use. Immunohistochemistry shows c-Met expression in an adenomatous polyp<sup>132</sup>. Laparoscopy visualizes the peritoneal cavity for minimally invasive surgery<sup>148</sup>. Endoscopy reveals a mucosal lesion (arrow) in gastric body<sup>106</sup>. Colonoscopy shows a large, 3-cm sigmoid polyp<sup>107</sup> (arrow). Otoscopy visualizes the eardrum and middle ear<sup>87</sup>. Ophthalmoscopy fundus camera image of the human retina<sup>110</sup>. Optical coherence tomography (OCT) allows microscopic cross-sectional imaging of the retina<sup>110</sup>. Middle row, Imaging technologies currently in clinical adoption phases. Diffuse optical tomography (DOT) shows oxygen saturation map for a breast with a 2.5-cm malignant tumor<sup>121</sup> (arrow). Speckle contrast image reveals meningeal artery (arrow) in the cortex and dura<sup>92</sup>. Fluorescence image shows colorectal polyps labelled with fluorescent peptides<sup>132</sup>. Fluorescence angiography shows loss of blood perfusion (arrow) in the foot<sup>133</sup>. Catheter OCT shows plaque rupture in a human coronary artery, identified by a broken fibrous cap<sup>113</sup> (arrow). Confocal laser endomicroscopy shows intramucosal bacteria (bright spots, inset) in the small intestine of a patient with ulcerative colitis<sup>126</sup>. Reflectance confocal microscopy shows an aggregate of neoplastic cells appearing as a focus of bright nuclei in the dermal–epidermal junction<sup>144</sup>. Bottom row, Technologies under development or in clinical testing. Microscopy of optically cleared thick-tissue blocks holds promise for the high-content mapping and phenotyping of normal and pathological tissue samples<sup>175</sup>. Functional connectivity maps of three sensory-motor networks generated with high-density DOT and fMRI (ref<sup>122</sup>). Intraoperative imaging of gliomas under white-light and fluorescence imaging with 5-aminolevulinic acid<sup>152</sup>. Multimodal (OCT plus fluorescence) image shows a three-dimensional rendering of the stented right iliac artery of a living rabbit<sup>117</sup>. Red, artery wall; white, stent; purple, thrombus; yellow, NIR fluorescent fibrin. Photoacoustic image of oxygen saturation of haemoglobin (sO<sub>2</sub>) in the murine brain vasculature. Clinically viable stimulated Raman microscopy shows hypercellularity and nuclear atypia of tumour, in

correspondence with conventional H&E microscopy<sup>138</sup>. Brillouin microscopy shows a longitudinal modulus map of the cornea in a keratoconus patient<sup>146</sup>. DOT image in the middle row courtesy of Qianqian Fang at Massachusetts General Hospital.

Author Manuscript

Author Manuscript

Author Manuscript

Author Manuscript

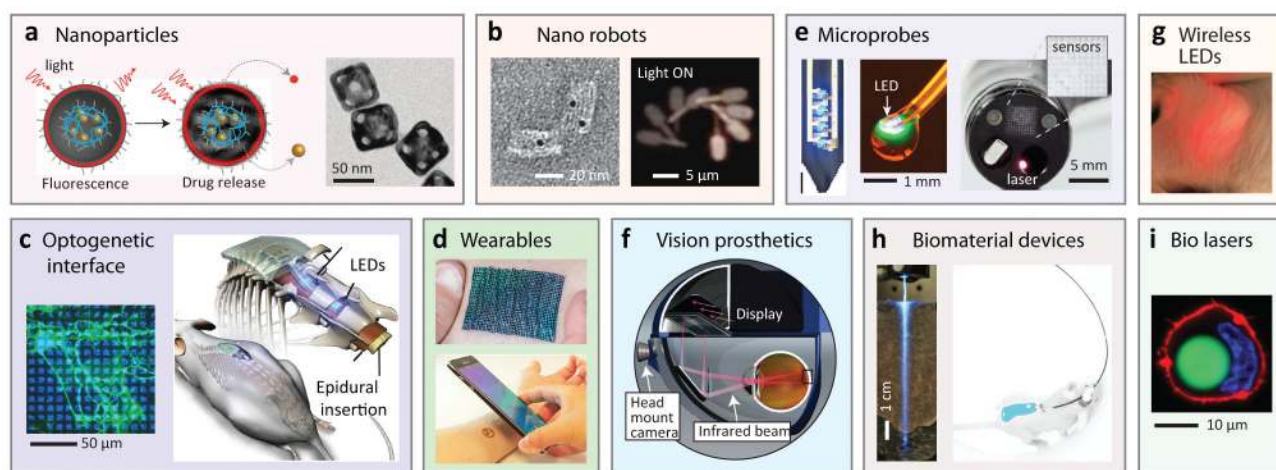


**Figure 5.**

Various implantable photonic devices at the proof-of-concept stage. **a**, Nanoparticles for drug delivery and treatment monitoring. Left, Light-activated drug release<sup>187</sup>. Right, photothermal-polymer-coated gold nanocages<sup>180</sup>. **b**, Nanorobots. Left, Transmission electron microscope image of an aptamer-gated DNA nanorobot capable of transporting 5-nm gold nanoparticles (black dots) to cells<sup>192</sup>. Right, Light-controllable microrobot with nanoscale phototactic machinery<sup>194</sup>. **c**, Optogenetic devices. Left, Optical pattern illuminated on cultured neuronal cells<sup>204</sup>. Right, Miniaturized, wireless, soft optoelectronic systems implanted in the spinal cord for performing optogenetics<sup>223</sup>. **d**, Wearables. Top, Thermo-chromic liquid-crystal-based temperature imaging device on the skin<sup>213</sup>. Bottom, Epidermal optoelectronic device powered by, and communicating with, a smartphone<sup>217</sup>. **e**, Microprobes. Left, Multifunctional, implantable optoelectronic device with LEDs and microelectrodes<sup>221</sup>. Middle, optoelectronic drug-delivery probe<sup>224</sup>. Right, multifunctional endoscope system based on transparent bioelectronic sensors and theranostic nanoparticles<sup>218</sup>. **f**, Vision prosthetics. Retinal prosthetic system using a head-mounted camera and a goggle, which projects NIR (880–915 nm) images to photodiode arrays implanted in the retina<sup>219</sup>. **g**, Wirelessly-powered, subcutaneously implanted LED in a mouse<sup>225</sup>. **h**, Biomaterial devices. Left, biodegradable polymer waveguide implanted in tissue for efficient light delivery<sup>229</sup>. Right, Fibre-pigtailed hydrogel waveguide implanted in a freely moving mouse for sensing and therapy<sup>212</sup>. **i**, Human cell containing an intracellular fluorescent-bead laser (green)<sup>232</sup>.



**Table 1**

Emerging medical applications of advanced optical technologies. Optical imaging and diagnostic technologies are increasingly less invasive, more accurate, molecular specific, cost effective and mobile. More surgical procedures will benefit from advanced optical imaging and optimized laser sources. Light-based therapies will integrate nanotechnologies and genetic technologies.

Area	Emerging applications
Diagnostic imaging	Non-invasive screening Super-resolution imaging Molecular diagnosis
Health monitoring	Point-of-care testing Implantable devices Mobile health
Surgery	Mobile health Robotic surgery Intraoperative optical biopsy
Therapy	Targeted therapy Precision medicine Optogenetics